Available online at www.sciencedirect.com
ScienceDirect
International Journal of Solids and Structures 44 (2007) 895–925
INTERNATIONAL JOURNAL OF SOLIDS and STRUCTURES
www.elsevier.com/locate/ijsolstr

Optimal shapes of contact interfaces due to sliding wear in the steady relative motion

I. Páczelt [a,*], Z. Mróz [b]

[a] Department of Mechanics, University of Miskolc, 3515 Miskolc Egyetemváros, Hungary
[b] Institute of Fundamental Technological Research, Warsaw, Poland

Received 25 January 2006; received in revised form 19 May 2006
Available online 26 May 2006

Abstract

The transient wear process at contact frictional interface of two elastic bodies in relative steady motion induces evolution of shape of the interface. A steady wear state may be reached with uniform wear rate and fixed contact surface shape. In this paper, the optimal contact shape is studied by formulating several classes of shape optimization problems, namely minimization of generalized wear volume rate, friction dissipation power and wear dissipation rate occurring in two bodies. The wear rule was assumed as a nonlinear dependence of wear rate on friction traction and relative sliding velocity, similar to the Archard rule. The wear parameters of two bodies may be different. It was demonstrated that different optimal contact shapes are generated depending on objective functional and wear parameters. When the uniform wear rate is generated at contact sliding surfaces, the steady state is reached. It was shown that in the steady state the wear parameters of two bodies cannot be independent of each other. The solution of nonlinear programming problem was provided by the iterative numerical procedure. It was assumed that the relative sliding velocity between contacting bodies results from translation and rotation of two bodies. In general, both regular and singular regimes of wear rate and pressure distribution may occur. The illustrative examples of drum brake, translating punch and rotating annular punch (disc brake) provide the distribution of contact pressure and wear rate for regular and singular cases associated with the optimality conditions. It is shown that minimization of the generalized wear dissipation rate provides solutions assuring existence of steady wear states.

Keywords: Sliding wear; Contact optimization; Steady wear state; *p*-Version of finite element method

1. Introduction

In engineering practice, mechanical and thermal interactions between machine or structural elements are frequently modeled as unilateral contact problems. The contact shape optimization is then usually aimed at minimizing the maximal contact pressure or effective stress. An extensive survey of contact pressure optimization problems was presented by Hilding et al. (1999) and by Haslinger and Neittaanmaki (1988). The papers by

* Corresponding author. Tel.: +36 46 565 162; fax: +36 46 565 163.
E-mail address: paczelt@freemail.hu (I. Páczelt).

0020-7683/$ - see front matter © 2006 Elsevier Ltd. All rights reserved.
doi:10.1016/j.ijsolstr.2006.05.027

Páczelt (2000) and Páczelt and Szabó (1994, 2002) provide solutions for 2D and 3D contact problems in which the pressure distribution is partially controlled. The application to roller bearings was presented in Páczelt and Szabó (2002), in Páczelt and Baksa (2002) with discretization of the domain with *p*-version finite elements, cf. Szabó and Babuska (1991), resulting in fast convergence and high order mapping assuring accurate geometry required for shape optimization.

However, in most engineering problems, when frictional slip and sliding occurs, the accompanying wear process induces variation of the contact surface shape and affects the contact pressure distribution. The initial shape and contact pressure vary during the wear process and evolve toward a steady state. This evolution can be simulated numerically by applying the wear rule specifying rate of wear in terms of relative slip velocity and contact pressure. A steady state could then be predicted by means of the incremental time integration procedure accounting for contact shape and pressure variation at each step. An alternative approach can also be considered by applying the variational procedure and searching for the optimal contact shape corresponding to extremum of an objective functional associated with the friction and wear process. It can be expected that for a properly selected objective functional the optimal shape is the same as that reached in the wear process. In other words, the wear process generates an *adaptive response* of the contact inducing optimal regime of interaction after an initial transient period. The knowledge of such optimal regimes is of fundamental importance for engineering applications by providing the methods of effective design and control of contact interfaces.

The present work is devoted to the analysis of evolution of shape of contact surface and pressure in the course of wear process. The analytical treatment of contact wear processes was presented in a book by Goryacheva and Dobuchin (1988). Numerical studies of elastic or thermoelastic wear problems were presented by Strömberg et al. (1996), Strömberg (1998), Páczelt and Pere (1999), Ireman et al. (2002). In general, there are several classes of problems. The first class occurs when within the contact domain there is an internal sticking zone where no friction slip occurs and an external slip zone where the relative slip induces displacement discontinuity. Under varying load action the wear process develops in the slip zone with accompanying shape evolution and progression of slip zone into the sticking zone. This wear mode, called the *fretting wear*, develops very slowly as there is no overall sliding at the contact interface. The numerical analysis of contact shape and pressure evolution by Johansson (1994) well illustrates this class of problems where the relative slip displacement is of order of elastic displacement. The second class of wear problems, called the *sliding wear*, occurs when the sliding of two contacting bodies occurs and is accompanied by the progressive wear process and contact shape evolution. For the translation elastic punch motion, the contact shape evolution was numerically analyzed by Marshek and Chen (1989), indicating uniform pressure and wear distribution in the steady state. The other class of problems is associated with *rolling wear*, typical in rail vehicle/track interaction when both slip and sticking zones develop consecutively at the contact.

In the previous work by Páczelt and Mróz (2005) the optimal shapes generated by wear process were analyzed by postulating minimization of the wear dissipation power and also the wear volume and the friction dissipation power. The physically most important criterion is that providing the uniform wear rate in the steady state of wear. It was shown that in the case of translatory and rotary motion the contact shape evolution tends to a steady state satisfying the minimum principle of the wear dissipation rate. On the other hand, minimization of friction dissipation power or wear volume rate provides different contact shapes, not satisfying the steady state property. In this paper, we shall extend the analysis of Páczelt and Mróz (2005) by deriving the optimality conditions with account for wear of two bodies and present the solutions for three cases, related to wear of drum braking system, wear of rotating tubular punch representing disk brake operation and wear of translating punch transferring resultant normal force and moment to the contact area. It is noted that for some parameter values the optimal solutions are *singular*, corresponding to localized contact zones at the perimeter or center line of the contact area. Both regular and singular optimal solutions are discussed and the physical relevance of minimum principle of the wear dissipation power is emphasized.

The paper is organized as follows. In Section 2 a brief exposition of contact problem is given with introduction of basic definitions and notations. Next, in Section 3 a brief formulation of wear rules of two contacting bodies with different wear parameters is presented. Section 4 provides the optimality conditions for the case of wear of two bodies and the necessary conditions of stationary states associated with different objective functions. Section 5 provides the analysis of two types of drum braking system. The aim of this section is to demonstrate the applicability of optimality conditions in numerical determination of optimal contact shapes in

sliding wear regimes and to clarify the character of regular, singular and near-singular solutions. Section 6 contains the solutions of optimal punch profiles interacting with plane contact. The effect of optimal shape sensitivity with respect to friction coefficient is clearly illustrated.

In Section 7 the optimality conditions for the case of wear of two rotating bodies and the steady state conditions are provided. The singular, near-singular and regular solutions are presented and the role of control parameter q is discussed. Section 8 summarizes the main results of the paper.

2. Contact problem

Without the restriction of generality, let us consider the contact problem (cf. for instance, Laursen, 2002; Wriggers, 2002) of two elastic bodies B_α ($\alpha = 1,2$) with the usual boundary and loading conditions. It will be assumed that the displacements and the deformations are small. On the boundary surface portion $S_u^{(\alpha)}$ the displacements $\mathbf{u}_0^{(\alpha)}$ are specified, on the $S_t^{(\alpha)}$ the traction vector $\mathbf{t}_0^{(\alpha)}$ is applied, and on the $S_c^{(\alpha)}$ the unilateral contact is expected. In this part of the bodies the boundary shape may be modified. The normal stress is $\sigma_n^{(\alpha)} = \mathbf{n}^{(\alpha)} \cdot \sigma^{(\alpha)} \cdot \mathbf{n}^{(\alpha)}$, where $\sigma^{(\alpha)}$ is the stress tensor, $\mathbf{n}^{(\alpha)}$ is the normal vector of the αth body along the surface $S_c^{(\alpha)} = \Omega$. The elastic displacements in the normal and tangential directions are denoted by $u_{e,n}^{(\alpha)}$ and $\mathbf{u}_{e,\tau}^{(\alpha)}$, their rates by $\dot{u}_{e,n}^{(\alpha)}$ and $\dot{\mathbf{u}}_{e,\tau}^{(\alpha)}$. The rigid body displacements are respectively $u_{R,n}^{(\alpha)}$ and $\mathbf{u}_{R,\tau}^{(\alpha)}$. After deformation the gap is $d = u_n^{(2)} - u_n^{(1)} + g$, where $u_n^{(\alpha)} = \mathbf{u}^{(\alpha)} \cdot \mathbf{n}_c$, $\mathbf{n}_c$ is the unit normal vector of contact surface and g is the initial gap (see Fig. 1) and the contact pressure $p = -\sigma_n^{(1)} = -\sigma_n^{(2)}$. In the normal direction the Signorini contact conditions are valid: there is contact if $d = 0$, $p \geqslant 0$, $x \in C$ and there is gap, if $d > 0$, $p = 0$, $x \in G$, i.e. $p \times d = 0$, $x \in \Omega = C \cup G$. The Coulomb dry friction condition and the non-associated sliding rule are the same as in the previous paper by Páczelt and Mróz (2005). They have been examined in detail in books by Laursen (2002) and Wriggers (2002).

Assume that the first body undergoes the rigid body motion, so that its translation and rotation with respect to a selected point C_0 is specified by vectors $\boldsymbol{\lambda}_F$ and $\boldsymbol{\lambda}_M$.

In this case the rigid body displacements in the normal and tangential directions are

$$u_{R,n}^{(1)} = (\boldsymbol{\lambda}_F + \boldsymbol{\lambda}_M \times \Delta\mathbf{r}) \cdot \mathbf{n}_c, \quad \mathbf{u}_{R,\tau}^{(1)} = (\boldsymbol{\lambda}_F + \boldsymbol{\lambda}_M \times \Delta\mathbf{r}) - u_{R,n}^{(1)}\mathbf{n}_c \tag{1}$$

where $\Delta\mathbf{r}$ is the position with respect to C_0.

The relative tangential velocity is calculated by the following formula

$$\dot{\mathbf{u}}_\tau = \dot{\mathbf{u}}_{e,\tau}^{(2)} - (\dot{\mathbf{u}}_{e,\tau}^{(1)} + \dot{\mathbf{u}}_{R,\tau}^{(1)}). \tag{2}$$

In the analysis of sliding wear process, usually the elastic portion of relative tangent velocity is much smaller than the rigid body motion induced velocity, thus

$$\|\dot{\mathbf{u}}_{e,\tau}^{(1)}\| + \|\dot{\mathbf{u}}_{e,\tau}^{(2)}\| \ll \|\dot{\mathbf{u}}_{R,\tau}^{(1)}\| \tag{3}$$

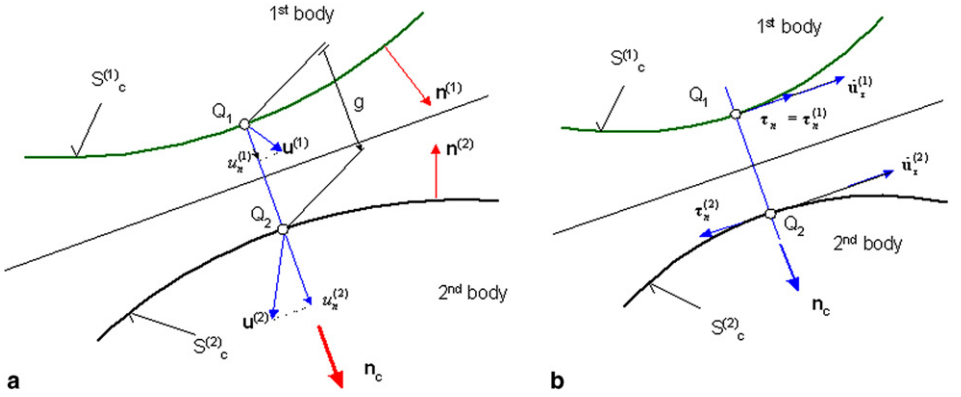

Fig. 1. Two bodies in contact: (a) definition of normal displacements $u_n^{(\alpha)}$ and the initial gap g, (b) tangential velocities $\dot{\mathbf{u}}_\tau^{(\alpha)}$ and contact shear stress $\boldsymbol{\tau}_n^{(\alpha)}$.

and the effect of elastic component of tangential relative velocity can be neglected in the wear analysis (see Páczelt and Mróz, 2005). We shall use this fact in our numerical study of wear process. The symbol $\|\cdot\|$ denotes the absolute value of the vector.

The boundary value problem is solved by variational principles using modified total potential energy with augmented Lagrangian technique (Wriggers, 2002; Páczelt, 2000). In our optimization problems it is supposed that the bodies are in contact on the whole sub-domain Ω_c of the contact zone $S_c = \Omega$. The temperature effects and heat generated at the frictional interface (see for instance Wriggers and Miehe, 1994; Strömberg et al., 1996; Strömberg, 1998; Páczelt and Pere, 1999; Ireman et al., 2002) in our investigation is neglected. In our consideration the wear is assumed as isotropic. Anisotropic friction and wear process has been investigated in papers Mróz and Stupkiewicz (1994), Johansson (1994) and Stupkiewicz and Mróz (1999).

The stationarity condition after discretization then provides the system of algebraic equations, which will be solved by the iterational Kalker procedure (see Kalker, 1985) with the control of the sign of the contact pressure. The contact conditions are checked at the Lobatto integration points of the contact elements during the solution process. The oscillations of contact pressure and displacements are minimized by using the node positioning and re-meshing technique described in Páczelt and Baksa (2002).

3. Formulation of the wear rule

In the wear process two main classes of problems can be distinguished. In the first class the contact domain S_c including the sticking and slip zones evolves in time. In the second class the domain S_c is fixed and the relative sliding occurs on S_c. We can next distinguish three sub-classes of problems. First, the wear rate is uniform over S_c and is steady in time. Second, the wear rate is not uniform over S_c but is steady in time. Third, the wear rate is not uniform over S_c and is varying in time. The steady state can be attained only in the first two sub-classes of problems. In this paper we will focus our discussion on the optimal contact shapes generated in the steady state of wear process and their numerical determination from the optimality conditions of objective functionals.

The shear stress in the contact surface is denoted by τ_n and calculated in terms of the contact pressure by the Coulomb friction law $\tau_n = \mu p_n$.

When the wear process occurs in two contacting bodies, the wear rule for the ith body is assumed in the form

$$\dot{w}_i = \beta_i(\tau_n)^{b_i}\|\dot{\mathbf{u}}_\tau\|^{a_i} = \beta_i(\mu p_n)^{b_i}\|\dot{\mathbf{u}}_\tau\|^{a_i} = \beta_i(\mu p_n)^{b_i} v_r^{a_i} = \tilde{\beta}_i p_n^{b_i} v_r^{a_i}, \quad i = 1,2 \tag{4}$$

where β_i, a_i, b_i are the wear parameters, μ is the coefficient of friction, $\tilde{\beta}_i = \beta_i \mu^{b_i}$, $v_r = \|\dot{u}_\tau\|$ is the relative velocity between two bodies. The wear parameters are assumed as constant, however, the state of contact interface evolves during the wear process, so these parameters may tend to their steady state values dependent on the surface and subsurface deformation.

A special case is of importance, namely the uniform wear rate (Goryacheva and Dobuchin, 1988; Páczelt and Mróz, 2005)

$$\dot{w} = \sum_{i=1}^{2} \dot{w}_i = \sum_{i=1}^{2} \beta_i(\mu p_n)^{b_i}\|\dot{\mathbf{u}}_\tau\|^{a_i} = \dot{w}_c = \text{const} \tag{5}$$

Assuming $b_1 = b_2 = b$, the contact pressure distribution can now be calculated from (5), namely

$$p_n = \left[\frac{\dot{w}_c}{\sum_{i=1}^{2}\beta_i \mu^b \|\dot{\mathbf{u}}_\tau\|^{a_i}}\right]^{\frac{1}{b}} \tag{6}$$

However, the slip velocity is in a general case unknown and should be determined from the solution of a specific case.

Note that in a steady state when the contact pressure distribution on S_c depends only on the position, the contact congruence requires that

$$\dot{w}_1/\dot{w}_2 = \text{const} \quad \text{or} \quad (p_n)^{(b_1-b_2)}(v_r)^{(a_1-a_2)} = \text{const} \tag{7}$$

4. Minimization of wear volume rate, friction dissipation power and wear dissipation power

Consider the wear process occurring in two contacting bodies. The first body in a form of punch B_1, moves relatively to the second body B_2 and remains in contact on the plane S_c. The punch B_1 is allowed to translate or rotate with respect to the body B_2 which is constrained and does not undergo rigid body motion (see Fig. 2). In the case of translation motion the relative sliding velocity v_r at the contact surface S_c is constant, in the case of rotation motion with respect to axis normal to the contact plane it equals $v_r = r\omega$, where r denotes the distance of a point on S_c from the axis of rotation. The wear volume rate at the contact surface S_c equals

$$\dot{W} = \int_{S_c} \dot{w}\,\mathrm{d}S = \int_{S_c} (\dot{w}_1 + \dot{w}_2)\,\mathrm{d}S = \sum_{i=1}^{2} \int_{S_c} \tilde{\beta}_i p_n^{b_i} v_r^{a_i}\,\mathrm{d}S \tag{8}$$

and the friction dissipation power is

$$D_F = \int_{S_c} \tau_n v_r\,\mathrm{d}S = \int_{S_c} \mu p_n v_r\,\mathrm{d}S \tag{9}$$

The wear dissipation power is specified from the following formula:

$$D_w = \int_{S_c} p_n \dot{w}\,\mathrm{d}S = \int_{S_c} p_n(\dot{w}_1 + \dot{w}_2)\,\mathrm{d}S = \int_{S_c} (\tilde{\beta}_1 p_n^{b_1+1} v_r^{a_1} + \tilde{\beta}_2 p_n^{b_2+1} v_r^{a_2})\,\mathrm{d}S \tag{10}$$

Consider now the new generalized forms of these functionals, already discussed by Páczelt and Mróz (2005) for the case of wear of one body. The generalized wear volume rate can be presented as follows:

$$\dot{W}^{(q)} = \sum_{i=1}^{2} \left(\int_{S_c} \dot{w}_i^q\,\mathrm{d}S \right)^{1/q} = \sum_{i=1}^{2} \left(\int_{S_c} (\tilde{\beta}_i p_n^{b_i} v_r^{a_i})^q\,\mathrm{d}S \right)^{1/q} = \sum_{i=1}^{2} A_i^{1/q} \tag{11}$$

the generalized friction dissipation power equals

$$D_F^{(q)} = \left(\int_{S_c} (\mu p_n v_r)^q\,\mathrm{d}S \right)^{1/q} = B^{1/q} \tag{12}$$

and the generalized wear dissipation power at the surface S_c is

$$D_w^{(q)} = \sum_{i=1}^{2} \left(\int_{S_c} (p_n \dot{w}_i)^q\,\mathrm{d}S \right)^{1/q} = \sum_{i=1}^{2} \left(\int_{S_c} (\tilde{\beta}_i p_n^{b_i+1} v_r^{a_i})^q\,\mathrm{d}S \right)^{1/q} = \sum_{i=1}^{2} C_i^{1/q} \tag{13}$$

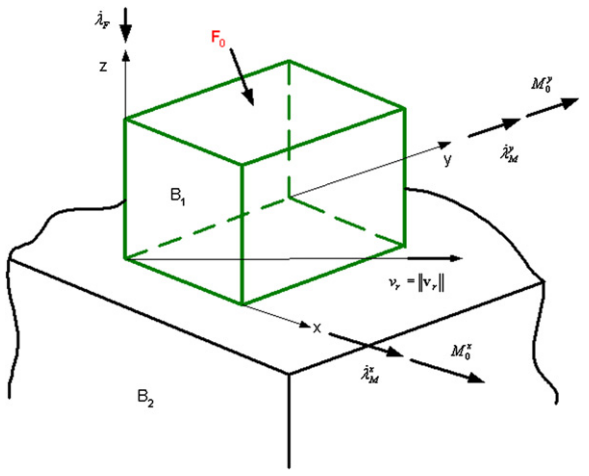

Fig. 2. The wear process occurring at contact interface of a punch moving with the relative velocity v_r and loaded by force $\mathbf{F}_0 = F_0^x \mathbf{e}_x + F_0^y \mathbf{e}_y - F_0 \mathbf{e}_z$ (with resulting moments M_0^x, M_0^y). The Lagrangian multipliers are $\dot{\lambda}_F$, $\dot{\lambda}_M^x$, $\dot{\lambda}_M^y$ and represent velocity components.

where q is called the *control parameter*. Let us note that for $q = 1$ these functionals represent global contact response measures such as friction or wear dissipation power and wear volume rate. For large values of q the functionals tend to local maximal values of integrands and provide control of local extremal responses at each contact point. The role of the parameter q is to regularize the optimization problem in order to avoid singular solutions.

In the following sections we shall analyze the minimum variational principles associated with these three functionals.

4.1. Variational principles in a stationary translation motion, v_r = const

In this case the relative velocity between two bodies $v_r = \text{const}$, as the second body B_2 is fixed, and the body B_1 moves with constant velocity. The translatory motion is in general combined with rotation relative to coordinate axes within the contact plane.

Assume the contact pressure $p_n(\mathbf{x})$ and friction stress $\mu p_n(\mathbf{x})$ to satisfy the global equilibrium conditions for the body B_1, so we have

$$\begin{aligned} \mathbf{f} &= -\int_{S_c} \mathbf{n}_c p_n \, dS + \mathbf{f}_0 = \mathbf{0}, \quad \mathbf{m} = -\int_{S_c} \Delta\mathbf{r} \times \mathbf{n}_c p_n \, dS + \mathbf{m}_0 = \mathbf{0} \\ \mathbf{f}_\tau &= \int_{S_c} \mathbf{e}_\tau \mu p_n \, dS + \mathbf{f}_{0\tau} = \mathbf{0}, \quad \mathbf{m}_\tau = \int_{S_c} \Delta\mathbf{r} \times \mathbf{e}_\tau \mu p_n \, dS + \mathbf{m}_{0\tau} = \mathbf{0} \end{aligned} \tag{14}$$

where $\mathbf{f}_0$, $\mathbf{f}_{0\tau}$ and $\mathbf{m}_0$, $\mathbf{m}_{0\tau}$ are resultant force and moment of normal and tangential tractions acting on body B_1, $\Delta\mathbf{r}$ is the position vector with respect to a reference point lying within the contact plane S_c, $\mathbf{e}_\tau$ is the tangential vector in the contact plane S_c. It is supposed that equations $\mathbf{f}_\tau = 0$, $\mathbf{m}_\tau = 0$ are satisfied automatically.

In the paper by Páczelt and Mróz (2005) the following minimization problems with equilibrium constraints were considered

Problem PW1: $\text{Min}\, \dot{W}^{(q)} = \dot{W}^{(q)}(p_n)$
Problem PW2: $\text{Min}\, D_F^{(q)} = D_F^{(q)}(p_n)$
Problem PW3: $\text{Min}\, D_w^{(q)} = D_w^{(q)}(p_n)$

$$\text{subject to } \left\{ \mathbf{f} = -\int_{S_c} \mathbf{n}_c p_n \, dS + \mathbf{f}_0 = \mathbf{0},\ \mathbf{m} = -\int_{S_c} \Delta\mathbf{r} \times \mathbf{n}_c p_n \, dS + \mathbf{m}_0 = \mathbf{0} \right\} \tag{15}$$

that is the objective function equal: $\dot{W}^{(q)}(p_n)$ or $D_F^{(q)}(p_n)$ or $D_w^{(q)}(p_n)$, the constraints are the equilibrium equations: $\mathbf{f} = \mathbf{0}$, $\mathbf{m} = \mathbf{0}$, and the local inequality for contact pressure is $p_n \geqslant 0$. The problems (15) are highly nonlinear.

Introducing the Lagrange multipliers $\dot{\boldsymbol{\lambda}}_F$ and $\dot{\boldsymbol{\lambda}}_M$, the Lagrangian functionals are

$$\begin{aligned} L_{\dot{W}}^{(q)} &= L_{\dot{W}}^{(q)}(p_n, \dot{\boldsymbol{\lambda}}_F, \dot{\boldsymbol{\lambda}}_M) = \dot{W}^{(q)}(p_n) + \dot{\boldsymbol{\lambda}}_F \cdot \mathbf{f} + \dot{\boldsymbol{\lambda}}_M \cdot \mathbf{m} \\ L_{D_F}^{(q)} &= L_{D_F}^{(q)}(p_n, \dot{\boldsymbol{\lambda}}_F, \dot{\boldsymbol{\lambda}}_M) = D_F^{(q)}(p_n) + \dot{\boldsymbol{\lambda}}_F \cdot \mathbf{f} + \dot{\boldsymbol{\lambda}}_M \cdot \mathbf{m} \\ L_{D_w}^{(q)} &= L_{D_w}^{(q)}(p_n, \dot{\boldsymbol{\lambda}}_F, \dot{\boldsymbol{\lambda}}_M) = D_w^{(q)}(p_n) + \dot{\boldsymbol{\lambda}}_F \cdot \mathbf{f} + \dot{\boldsymbol{\lambda}}_M \cdot \mathbf{m} \end{aligned} \tag{16}$$

Requiring the variations of functionals to vanish, we obtain the formulae specifying the contact pressure distribution, namely

$$\delta L_{\dot{W}}^{(q)} = 0 \Rightarrow p_n = \left(\frac{\dot{\boldsymbol{\lambda}}_F \cdot \mathbf{n}_c + (\dot{\boldsymbol{\lambda}}_M \times \Delta\mathbf{r}) \cdot \mathbf{n}_c}{b_1 (\tilde{\beta}_1 v_r^{a_1})^q A_1^{\frac{1-q}{q}} + b_2 (\tilde{\beta}_2 v_r^{a_2})^q A_2^{\frac{1-q}{q}} p_n^{q(b_2-b_1)}} \right)^{\frac{1}{b_1 q - 1}} \tag{17}$$

In Eq. (17) the term $f = \dot{\boldsymbol{\lambda}}_F \cdot \mathbf{n}_c + (\dot{\boldsymbol{\lambda}}_M \times \Delta\mathbf{r}) \cdot \mathbf{n}_c$ is a linear function of position coordinates $\Delta\mathbf{r}$, the integrated values A_i $i = 1, 2$ depend on pressure p_n and relative velocity v_r. Let us denote the terms of denominator by $Q_i = b_i (\tilde{\beta}_i v_r^{a_{ii}})^q A_i^{\frac{1-q}{q}}$, next by $s = b_1 q - 1$ and $m = q(b_2 - b_1)$. The contact pressure now is

$$p_n = \left(\frac{f}{Q_1 + Q_2 p_n^m}\right)^{\frac{1}{s}} \quad \text{if } s = b_1 q - 1 \neq 0 \tag{18}$$

that is

$$p_n^s = \frac{f}{Q_1 + Q_2 p_n^m} = \frac{f/Q_1}{1 + p_n^m Q_2/Q_1} = \frac{f}{Q_1}\left(1 + p_n^m \frac{Q_2}{Q_1}\right)^{-1} \cong \frac{f}{Q_1}\left(1 - p_n^m \frac{Q_2}{Q_1}\right)$$

and

$$p_n^s + f\frac{Q_2}{Q_1^2} p_n^m \cong \frac{f}{Q_1} \tag{19}$$

When $m \neq 0$, the contact pressure cannot be expressed as a homogeneous function of f. In fact, the right hand side is a linear function of position, on the left hand side the second term may be linear only when $m = 0$. Thus, a physically correct solution is reached when

$$b_1 = b_2 = b. \tag{20}$$

Let us note that (20) is also the contact congruence condition $\dot{w}_1/\dot{w}_2 = \text{const}$.

In this case we have

$$p_n = \left(\frac{\dot{\boldsymbol{\lambda}}_{\mathrm{F}} \cdot \mathbf{n}_{\mathrm{c}} + (\dot{\boldsymbol{\lambda}}_M \times \Delta\mathbf{r}) \cdot \mathbf{n}_{\mathrm{c}}}{b(\tilde{\beta}_1 v_r^{a_1})^q A_1^{\frac{1-q}{q}} + b(\tilde{\beta}_2 v_r^{a_2})^q A_2^{\frac{1-q}{q}}}\right)^{\frac{1}{bq-1}} \quad \text{if } bq \neq 1 \tag{21}$$

For Problem PW2 we have

$$\delta L_{D_{\mathrm{F}}}^{(q)} = 0 \Rightarrow p_n = \left(\frac{\dot{\boldsymbol{\lambda}}_{\mathrm{F}} \cdot \mathbf{n}_{\mathrm{c}} + (\dot{\boldsymbol{\lambda}}_M \times \Delta\mathbf{r}) \cdot \mathbf{n}_{\mathrm{c}}}{(\mu v_r)^q B^{\frac{1-q}{q}}}\right)^{\frac{1}{q-1}} \quad \text{if } q \neq 1 \tag{22}$$

and for Problem PW3, similar to Problem PW1 assuming $b_1 = b_2 = b$, there is

$$\delta L_{D_{\mathrm{w}}}^{(q)} = 0 \Rightarrow p_n = \left(\frac{\dot{\boldsymbol{\lambda}}_{\mathrm{F}} \cdot \mathbf{n}_{\mathrm{c}} + (\dot{\boldsymbol{\lambda}}_M \times \Delta\mathbf{r}) \cdot \mathbf{n}_{\mathrm{c}}}{(b+1)\left[(\tilde{\beta}_1 v_r^{a_1})^q C_1^{\frac{1-q}{q}} + (\tilde{\beta}_2 v_r^{a_2}) C_2^{\frac{1-q}{q}}\right]}\right)^{\frac{1}{(b+1)q-1}} \quad \text{if } (b+1)q \neq 1 \tag{23}$$

and the equilibrium equations $\mathbf{f} = \mathbf{0}$, $\mathbf{m} = \mathbf{0}$. The Lagrangian multipliers, next the rigid body motion velocities $\dot{\boldsymbol{\lambda}}_{\mathrm{F}}$, $\dot{\boldsymbol{\lambda}}_M$ can be calculated from the equilibrium equations, then from (4) and (8) we specify the wear rate, and the wear volume rate. It is important, that the contact pressure (21)–(23) must be positive over S_{c}. Otherwise, the actual contact region will vary in the wear process so we would have a non-steady state of wear process. In our investigation it is assumed, that the Signorini normal contact conditions are satisfied, then $p_n \geqslant 0$, $d \geqslant 0$, $p_n d = 0$ when the initial gap is calculated. The optimal gap between bodies can be easily calculated by means of the iteration process, described in Appendix C of the previous paper of Páczelt and Mróz (2005).

The following important conclusion is stated. *A steady state wear process for two bodies in translation motion is reached only when the wear parameters b_i are equal, $b_1 = b_2 = b$ in the modified Archard model* $\dot{w}_i = \tilde{\beta}_i p_n^{b_i} v_r^{a_i}$ $i = 1, 2$.

4.1.1. Discussion of special cases

4.1.1.1. Uniform translation. In paper by Páczelt and Mróz (2005) this case was considered when the contact normal at each point of S_{c} is parallel to coordinate axis z, that is $\mathbf{n}_{\mathrm{c}} = -\mathbf{e}_z$. In the first case, the resultant load vector is $\mathbf{f}_0 = -F_0\mathbf{e}_z$, the velocity in the direction of z is $\dot{\boldsymbol{\lambda}}_{\mathrm{F}} \cdot \mathbf{n}_{\mathrm{c}} = \dot{\lambda}_{\mathrm{F}}$ and the rotational angular velocity $\dot{\boldsymbol{\lambda}}_M = 0$. We conclude that three minimization problems provide the same result, that is if the contact region S_{c} does not vary in the wear process, then the contact pressure is constant ($p_n = F_0/S_{\mathrm{c}}$) and the local wear rate equals $\dot{w} = \sum_{i=1}^{2} (F_0/S_{\mathrm{c}})^b \tilde{\beta}_i v_r^{a_i} = \text{const1}$ with the wear volume rate equal to $\dot{W} = \sum_{i=1}^{2} \tilde{\beta}_i v_r^{a_i} F_0^b S_{\mathrm{c}}^{1-b} = \text{const2}$, that is

the wear volume rate depends only on a value of the resultant force F_0. If the wear parameters $b_1 \neq b_2$ the wear process cannot evolve to constant pressure over the contact domain, that is the wear process cannot reach the steady state.

4.1.1.2. Translation and rotation of punch B_1. The body B_1 is assumed to undergo a rigid body translation and rotation with respect to the axes lying in the contact x, y plane. In this case the translation and angular velocities are $\dot{\boldsymbol{\lambda}}_{\mathrm{F}} = -\dot{\lambda}_{\mathrm{F}}\mathbf{e}_z$, $\dot{\boldsymbol{\lambda}}_M = \dot{\lambda}_M^x\mathbf{e}_x + \dot{\lambda}_M^y\mathbf{e}_y$, the resultant force and moment are $\mathbf{f}_0 = -F_0\mathbf{e}_z$, $\mathbf{m}_0 = M_0^x\mathbf{e}_x + M_0^y\mathbf{e}_y$ and the position vector is $\Delta\mathbf{r} = x\mathbf{e}_x + y\mathbf{e}_y$. The Lagrangian multipliers $\dot{\lambda}_{\mathrm{F}}$, $\dot{\lambda}_M^x$, $\dot{\lambda}_M^y$ are determined from the equilibrium equations which can be written in the following collective form

$$\mathbf{f}_{\dot{W},D_{\mathrm{F}},D_{\mathrm{w}}} = \mathbf{f}_{\dot{W},D_{\mathrm{F}},D_{\mathrm{w}}}(p_n, \dot{\lambda}_{\mathrm{F}}, \dot{\lambda}_M^x, \dot{\lambda}_M^y) \tag{24}$$

This nonlinear equation may be solved by the Newton–Raphson technique. After solution of (24) it is possible to calculate the final distribution of contact pressure, wear rate and from integral (8) the volume wear rate. It was proved by Páczelt and Mróz (2005) that for $b = 1$, $q = 1$ and $\mathbf{n}_{\mathrm{c}} = -\mathbf{e}_z$ the optimal contact pressure is linearly distributed on the contact surface. When only translatory motion occurs, then the pressure is uniformly distributed.

5. Application of optimality conditions: drum braking system

5.1. Regular optimal regimes

Consider now a specific case, namely, the elastic breaking shoe interacting with the rotating cylinder, Fig. 3. The present configuration is also used in experimental investigation of wear as the so called block-on- ring test, cf. Kim et al. (2005). The sliding velocity is now constant on the contact surface S_{c}. The shoe is loaded uniformly by the pressure $\tilde{p}$ resulting in the force F_0 acting on the cylinder. The thickness of brake system is equal to t.

In this case contact normal, load vector, and rigid body velocity are

$$\mathbf{n}_{\mathrm{c}} = -\sin\alpha\mathbf{e}_x - \cos\alpha\mathbf{e}_z, \quad \mathbf{f}_0 = -F_0\mathbf{e}_z, \quad \dot{\boldsymbol{\lambda}}_{\mathrm{F}} \cdot \mathbf{n}_{\mathrm{c}} = \dot{\lambda}_{\mathrm{F}} \cdot \cos\alpha \tag{25}$$

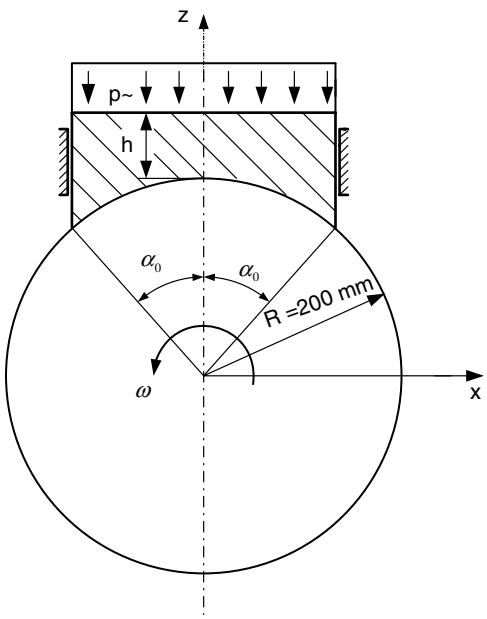

Fig. 3. Brake system, load and geometrical parameters.

It is supposed that there is no wear in the second body. Using the following notations $a = a_1$, $\tilde{\beta} = \tilde{\beta}_1$, $A = A_1$, $C = C_1$, from the stationarity conditions (21)–(23) we obtain the formulae specifying the contact pressure distributions, namely

$$\delta L^{(q)}_{\dot{W}} = 0 \Rightarrow p_n = \left(\frac{\dot{\lambda}_{\mathrm{F}} \cdot \cos\alpha}{b(\tilde{\beta} v_r^a)^q A^{\frac{1-q}{q}}}\right)^{\frac{1}{bq-1}} \quad \text{if } bq \neq 1 \tag{26}$$

$$\delta L^{(q)}_{D_{\mathrm{F}}} = 0 \Rightarrow p_n = \left(\frac{\dot{\lambda}_{\mathrm{F}} \cdot \cos\alpha}{(\mu v_r)^q B^{\frac{1-q}{q}}}\right)^{\frac{1}{q-1}} \quad \text{if } q \neq 1 \tag{27}$$

$$\delta L^{(q)}_{D_{\mathrm{w}}} = 0 \Rightarrow p_n = \left(\frac{\dot{\lambda}_{\mathrm{F}} \cdot \cos\alpha}{(b+1)(\tilde{\beta} v_r^a)^q C^{\frac{1-q}{q}}}\right)^{\frac{1}{(b+1)q-1}} \quad \text{if } (b+1)q \neq 1 \tag{28}$$

From the equilibrium equations we obtain the expressions for the Lagrange multiplier $\dot{\lambda}_{\mathrm{F}}$, thus

$$\min \dot{W} \Rightarrow \dot{\lambda}_{\mathrm{F}} = F_0^{bq-1} b(\tilde{\beta} v_r^a)^q A^{\frac{1-q}{q}} \left(\int_{-\alpha_0}^{\alpha_0} (\cos\alpha)^{\frac{1}{bq-1}} Rt \,\mathrm{d}\alpha\right)^{1-bq} \tag{29}$$

$$\min D_{\mathrm{F}} \Rightarrow \dot{\lambda}_{\mathrm{F}} = F_0^{q-1} (\mu v_r)^q B^{\frac{1-q}{q}} \left(\int_{-\alpha_0}^{\alpha_0} (\cos\alpha)^{\frac{1}{q-1}} Rt \,\mathrm{d}\alpha\right)^{1-q} \tag{30}$$

$$\min D_{\mathrm{w}} \Rightarrow \dot{\lambda}_{\mathrm{F}} = F_0^{(b+1)q-1} (b+1)(\tilde{\beta} v_r^a)^q C^{\frac{1-q}{q}} \left(\int_{-\alpha_0}^{\alpha_0} (\cos\alpha)^{\frac{1}{(b+1)q-1}} Rt \,\mathrm{d}\alpha\right)^{1-(b+1)q} \tag{31}$$

In view of (26)–(31) the contact pressure is expressed as follows:

$$\min \dot{W} \Rightarrow p_n = \left(\frac{F_0}{\int_{-\alpha_0}^{\alpha_0} (\cos\alpha)^{\frac{1}{bq-1}} Rt \,\mathrm{d}\alpha}\right) (\cos\alpha)^{\frac{1}{bq-1}} \tag{32}$$

$$\min D_{\mathrm{F}} \Rightarrow p_n = \left(\frac{F_0}{\int_{-\alpha_0}^{\alpha_0} (\cos\alpha)^{\frac{1}{q-1}} Rt \,\mathrm{d}\alpha}\right) (\cos\alpha)^{\frac{1}{q-1}} \tag{33}$$

$$\min D_{\mathrm{w}} \Rightarrow p_n = \left(\frac{F_0}{\int_{-\alpha_0}^{\alpha_0} (\cos\alpha)^{\frac{1}{(b+1)q-1}} Rt \,\mathrm{d}\alpha}\right) (\cos\alpha)^{\frac{1}{(b+1)q-1}} \tag{34}$$

Let us note that the contact pressure is non-uniform on S_{c}. It becomes uniform when $q \to \infty$.

The volume wear rate associated with three functionals $\dot{W}$, D_{F} and D_{w} is

$$\min \dot{W} \Rightarrow \frac{\dot{W}}{\tilde{\beta} v_r^a F_0^b} = \left(\frac{\int_{-\alpha_0}^{\alpha_0} (\cos\alpha)^{\frac{b}{bq-1}} Rt \,\mathrm{d}\alpha}{\left(\int_{-\alpha_0}^{\alpha_0} (\cos\alpha)^{\frac{1}{bq-1}} Rt \,\mathrm{d}\alpha\right)^b}\right) \tag{35}$$

$$\min D_{\mathrm{F}} \Rightarrow \frac{\dot{W}_{D_{\mathrm{F}}}}{\tilde{\beta} v_r^a F_0^b} = \left(\frac{\int_{-\alpha_0}^{\alpha_0} (\cos\alpha)^{\frac{b}{q-1}} Rt \,\mathrm{d}\alpha}{\left(\int_{-\alpha_0}^{\alpha_0} (\cos\alpha)^{\frac{1}{q-1}} Rt \,\mathrm{d}\alpha\right)^b}\right) \tag{36}$$

$$\min D_{\mathrm{w}} \Rightarrow \frac{\dot{W}_{D_{\mathrm{w}}}}{\tilde{\beta} v_r^a F_0^b} = \left(\frac{\int_{-\alpha_0}^{\alpha_0} (\cos\alpha)^{\frac{b}{(b+1)q-1}} Rt \,\mathrm{d}\alpha}{\left(\int_{-\alpha_0}^{\alpha_0} (\cos\alpha)^{\frac{1}{(b+1)q-1}} Rt \,\mathrm{d}\alpha\right)^b}\right) \tag{37}$$

The frictional dissipation power now is expressed in the form

$$D_{\mathrm{F}} = \int_{-\alpha_0}^{\alpha_0} \mu p_n v_r Rt \,\mathrm{d}\alpha = v_r \mu \int_{-\alpha_0}^{\alpha_0} p_n Rt \,\mathrm{d}\alpha = v_r \mu F_0 \tag{38}$$

5.2. Analysis of singular solutions

To discus in more detail the types of singular solutions, consider first the problem of min $\dot{W}$. When $bq \to 1$ the pressure and wear distribution is localized either at the center or at the edge of ring shoe. In fact, we have two different singular solutions, namely

$bq > 1$ and $bq \to 1$ – contact pressure localization at $\alpha = 0$,
$bq < 1$ and $bq \to 1$ – contact pressure localization at $\alpha = \pm\alpha_0$

because according to (32) there is

$$\frac{p_n}{p_{n0}} = \left(\frac{\cos\alpha}{\cos 0}\right)^{\frac{1}{bq-1}} \quad \text{and} \quad \frac{p_n}{p_{nb}} = \left(\frac{\cos\alpha_0}{\cos\alpha}\right)^{\frac{1}{1-bq}}, \tag{39}$$

where $p_{n0} = p_n(\alpha = 0)$, $p_{nb} = p_n(\alpha = \pm\alpha_0)$.

Similarly for the problem min D_F, we have two different singular solutions for $q > 1$ and $q \to 1$ next $q < 1$ and $q \to 1$.

For the problem min D_w different singularities occur for $(b+1)q > 1$ and $(b+1)q \to 1$, next for $(b+1)q < 1$ and $(b+1)q \to 1$.

Obviously, for engineering applications, the uniform wear contact profile is most important.

5.3. Drum braking system 1: Numerical study of extremum principles

Referring to Fig. 3, consider the interaction of the break shoe with the rotating drum. The shoe is loaded by the uniform pressure $\tilde{p}$ with the resultant force $F_0 = 10$ kN. The contact angle is $\alpha_0 = \pm 30°$, the drum radius equals $R = 200$ mm, the thickness is $t = 10$ mm.

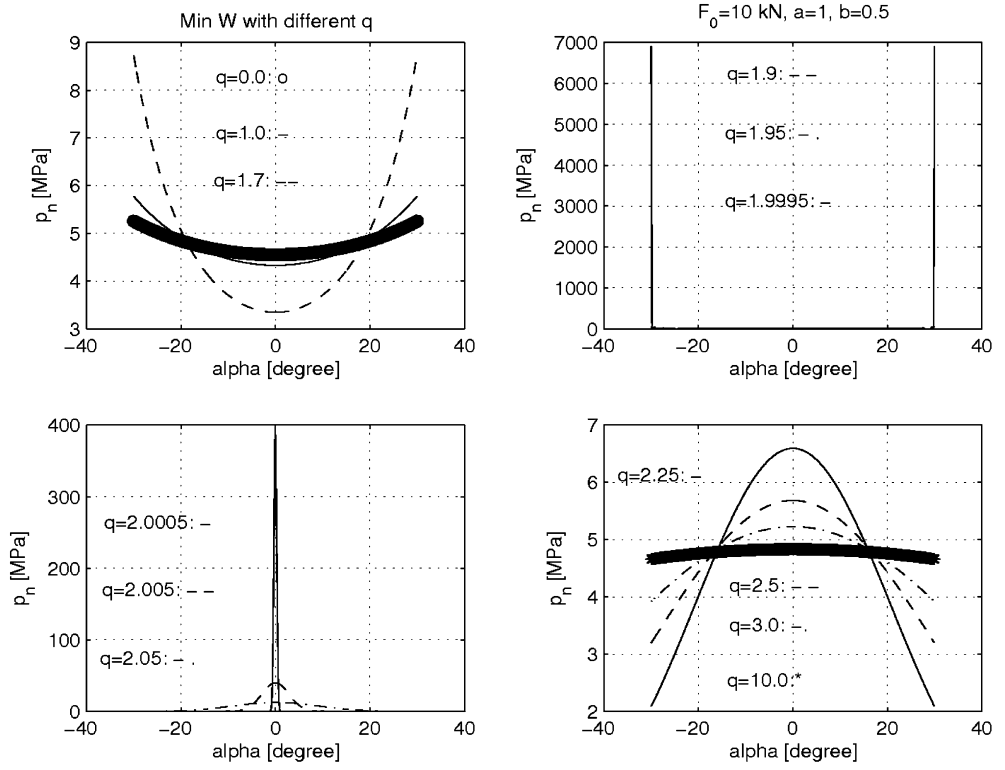

Fig. 4. Distribution of contact pressure by using the principle min $\dot{W}$ for wear parameters $a = 1$, $b = 0.5$ and different values of q.

It is supposed that elements of the brake system are in the plane stress state. The brake shoe may translate along the z-axis and engage the drum. The wear parameter equals $\beta = 0.0002$, the frictional coefficient is $\mu = 0.25$, the angular velocity of the disk equals $\omega = 2.5$ rad/s.

The analysis provides the distribution of contact pressure and wear rate predicted by the optimality conditions (32)–(37) associated with the functionals $\dot{W}$, D_F and D_w. Figs. 4 and 5 provide the pressure and wear distribution corresponding to the extremum of wear volume rate $\dot{W}$ at $a = 1.0$, $b = 0.5$ and different values of q varying between $q = 0.0$ and $q = 10.0$.

It is seen that for q close to 2 the contact pressure and wear distribution is highly localized in the border portion of contact area or in the center region. For increasing q the pressure and wear distribution becomes more uniform. In fact, the uniform distribution is obtained for $q \to \infty$, that is for minimization of the highest value of local wear rate generated by the integral functional (8).

Differing results are obtained by minimizing D_F and D_w. Fig. 6 presents the optimal distributions of contact pressure for increasing values of q and $a = 1$, $b = 0.5$ obtained from the condition of $\min D_F$. It is seen that the localized distribution of contact pressure in the central portion of contact occurs for q close to 1.0 tends a nearly uniform distribution for $q = 10.0$. Fig. 7 presents the optimal wear rate distributions for the condition $\min D_w$. The singular solution can be reached at $q \to 2/3$ and $2/3 \leftarrow q$. The optimal solution tends to uniform pressure and wear for increasing values of q.

The present study indicates that minimization of the total wear volume rate or dissipation rate may lead to localized quasi singular distributions for which no steady wear state will be reached. The uniform distribution is predicted for $q \to \infty$, that is for minimization of maximal local values of wear rate or dissipation rates. Noting that optimal distributions for the objective integrals (35)–(37) are specified by the expressions

$$(\cos\alpha)^{\frac{b}{bq-1}}, \quad (\cos\alpha)^{\frac{b}{q-1}}, \quad (\cos\alpha)^{\frac{b}{(b+1)q-1}}$$

it is seen that the condition $\min D_w$ provides the fastest evolution toward uniform distribution for increasing values of q.

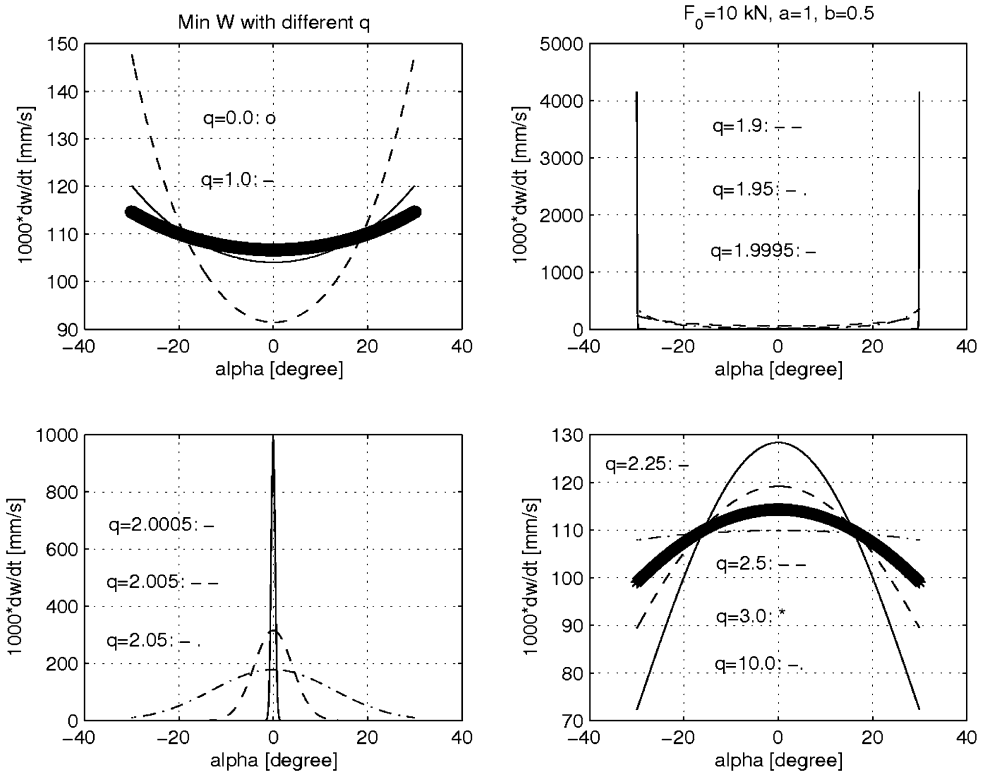

Fig. 5. Distribution of wear rate by using the principle $\min \dot{W}$ for wear parameters $a = 1$, $b = 0.5$ and different values of q.

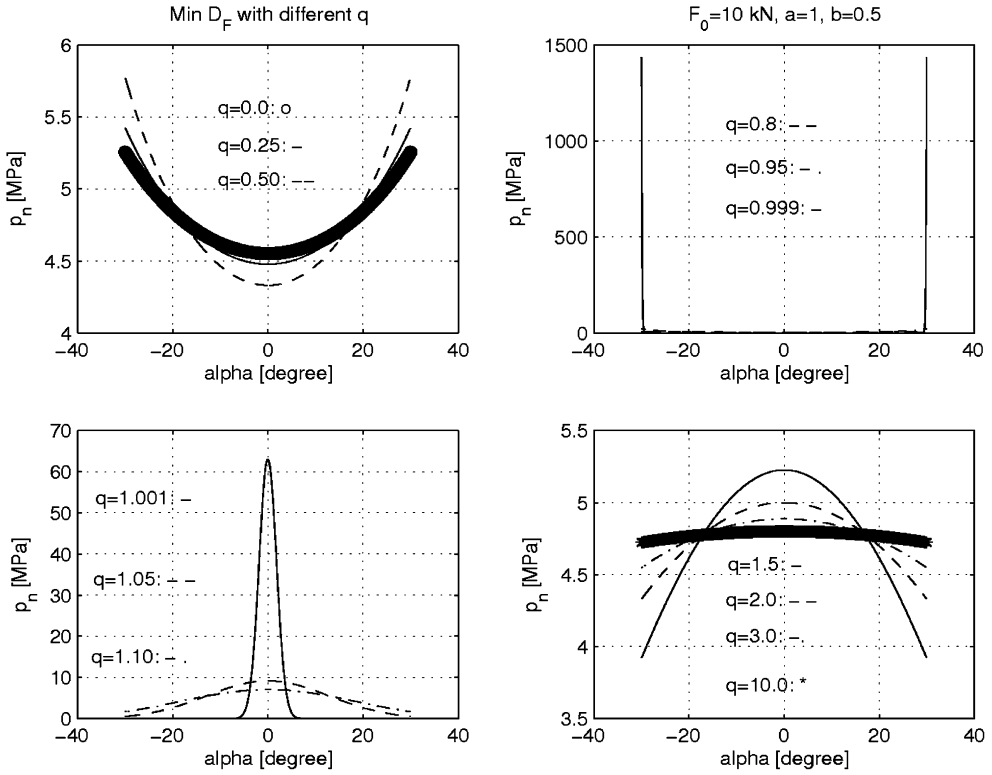

Fig. 6. Distribution of contact pressure by using the principle min D_F, wear parameters $a = 1$, $b = 0.5$, and varying q.

Let us now investigate the optimal gap in the brake system of Fig. 3. The material of all parts of the system is linear, Young modulus $E = 2.1$ MPa, Poisson ratio $v = 0.3$. The thickness is 10 mm, the load pressure equals $\tilde{p} = 5$ MPa, that is the load resultant force $F_0 = 10$ kN. The coefficient of friction $\mu = 0.25$, angular velocity of the disk equals $\omega = 2.5$ rad/s. The elastic disk rotates in the anti clockwise direction. First, it is assumed that there is no initial gap and the contact boundary of the shoe has cylindrical form. The height of shoe is $h = 100$ mm.

Using the p-version of finite element technique for the solution of optimization contact problem with control of contact pressure (see Páczelt, 2000; Páczelt and Baksa, 2002; Páczelt and Mróz, 2005) the uniform contact pressure distribution is reached for a small gap introduced with respect to the initial cylindrical form. In the original configuration is not gap present. At the edge of contact zone we obtain the singular solution, with the normal stress concentration at a very high level. We note also that there is asymmetry in stress distribution in the case of friction contact. Fig. 8a and b presents the calculated optimal initial gap (variation of contact surface of shoe in radial direction, that is the form reached in a steady state of wear process). In the case of frictionless contact ($\mu = 0$), the optimal gap has a form symmetrical with respect to z-axis. In the case of frictional contact, the optimal gap is asymmetrical, with higher values near the leading edge of the shoe. The analysis illustrates, that the effect of friction on contact shape is very important. In Fig. 8 b it is shown that very small friction coefficient ($\mu = 0.005$) induces significant shape variation with respect to frictionless shape.

5.4. Drum braking system 2

Consider now the drum braking system for which the shoe is of constant thickness ring form and the distributed load is concentrated at the shoe center with uniformly vertical traction $\tilde{p} = 59.58336$ MPa. The resultant force is $F_0 = 10$ kN. Fig. 9 presents the finite element mesh for a half part of the brake.

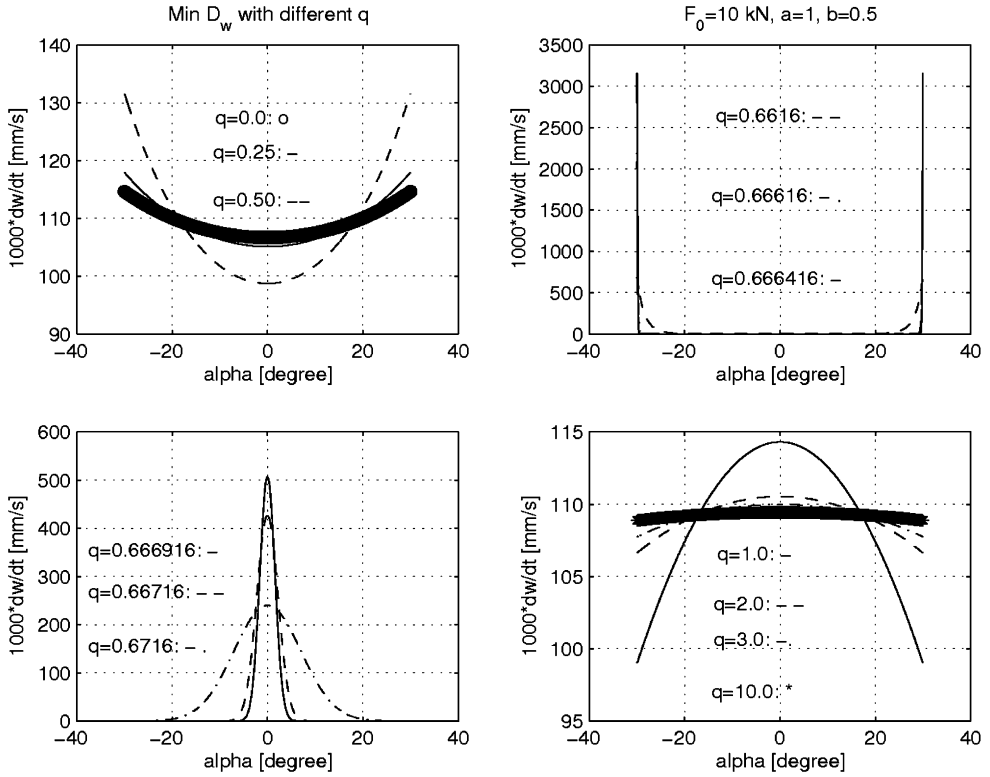

Fig. 7. Distribution of wear rate by using the principle $\min D_w$, wear parameters $a = 1$, $b = 0.5$, and varying q.

The initial contact pressure distribution is shown in Fig. 10. It is seen that it is highly localized near the center line and due to friction on the left side boundary. The optimal form of contact is reached in steady state of wear process, when the contact pressure becomes uniform, $p_n = 5.028$ MPa. The optimal shapes of contact surface are presented in Fig. 11 for different values of friction coefficient. The contact forms are not symmetric with respect to the central line due to friction effect at the interface. The shape of upper body can be calculated by applying the special iteration process (for details, see Appendix of Páczelt and Mróz (2005) modified according to the present Appendix A).

The solution presented in Fig. 11a was obtained for the case of two side constraint at $x = 100$ and $x = -100$, where the tangential displacement $u = 0$. The alternative solutions can be presented for the cases when only the left or right side boundary is constrained, that is $u = 0$ at $x = -100$ or $x = 100$. The central constraint: $u = 0$ for $x = 0$ corresponds to different solution. The optimal wear profiles for two side, one side and central constraints are shown in Fig. 11b. It is seen that there is a strong effect of disc constraint. In the case of the left side constraint the load is uniform along the upper boundary surface of the shoe: $\tilde{p} = 5$ MPa.

6. Translation of plane punch transferring normal force and moment

Consider now the case when the translating punch transfers contact pressure characterized by the resultant normal force and the moment with respect to the center contact line. For simplicity, consider the plane elastic punch (body B_1) in the x, z-plane translating along the elastic plate (body B_2) of the same elastic parameters. In Fig. 12 the punch dimensions and the finite element mesh are shown.

The wear parameters are: $\beta = 2 \times 10^{-4}$, $a = 1$, $b = 2$, $q = 1$, the relative velocity along the x-axis is $v_r = 5$ mm/s, the vertical load $F_0 = 1$ kN, its moment with respect to the center point $x = 0$, $z = 100$ mm varies within the range -5 kN mm $\leqslant M_0 = M_0^y \leqslant 5$ kN mm assuring positive contact pressure within the whole contact area. Applying the optimality conditions (23), we have

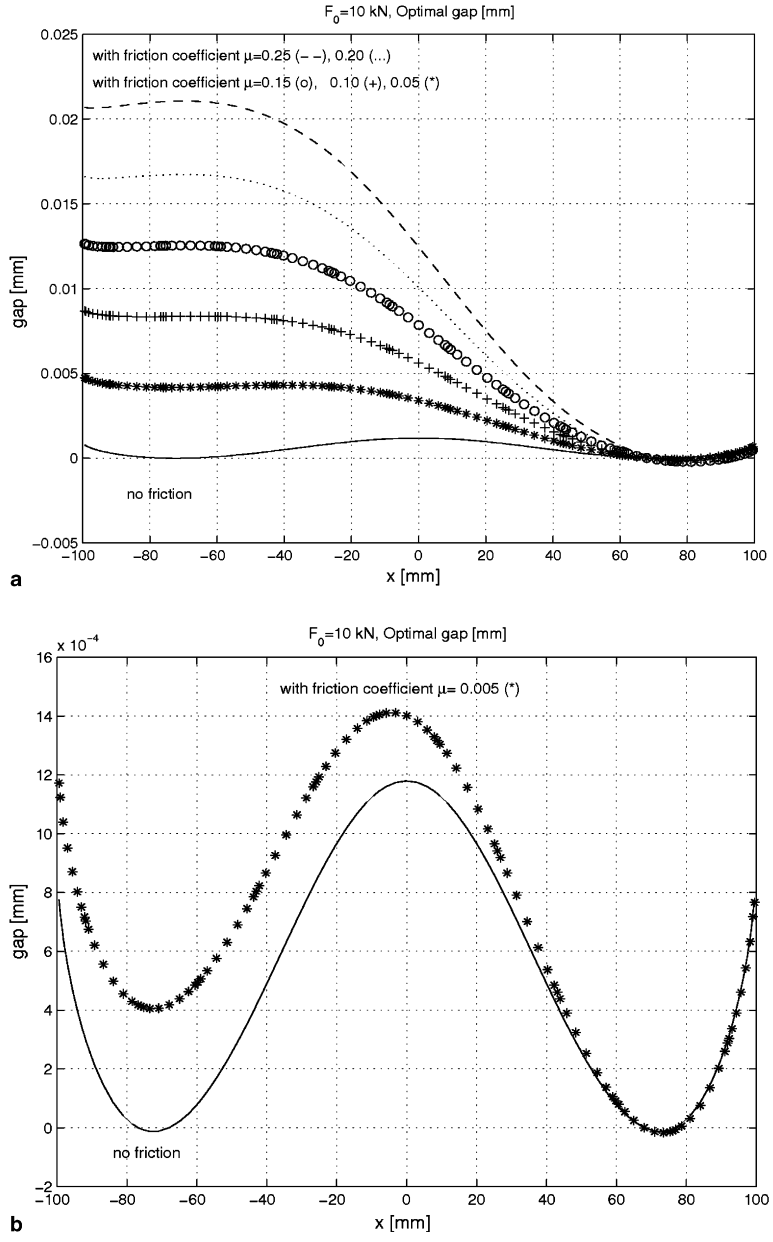

Fig. 8. Optimal gap (in the radial direction) generating constant pressure distribution for $p_n = \sim 5$ MPa between the bodies with the different values of friction coefficient (steady state of wear process in the friction case): (a) variation of optimal shape for increasing friction coefficients, (b) the effect of small friction on optimal shape.

$$p_n = \left(\frac{\dot{\lambda}_{\mathrm{F}} + \dot{\lambda}_M x}{(b+1)(\tilde{\beta} v_r^a)^q C^{\frac{1-q}{q}}} \right)^{\frac{1}{(b+1)q-1}} \tag{40}$$

and from the equilibrium equations $f = 0$, $m_y = 0$, the multipliers $\dot{\lambda}_{\mathrm{F}}$, $\dot{\lambda}_M$ can be calculated using the Newton–Raphson iteration procedure.

Fig. 13 presents the variation of multipliers for the constant normal force and varying moment value. The multipliers are proportional to translation and rotation velocities of the punch. Thus, at the upper boundary we have the displacement components: at $z = 200$ mm: $u = 0$, $w = -(\dot{\lambda}_{\mathrm{F}} + \dot{\lambda}_M x) d_{\mathrm{w}}$, and constraint conditions

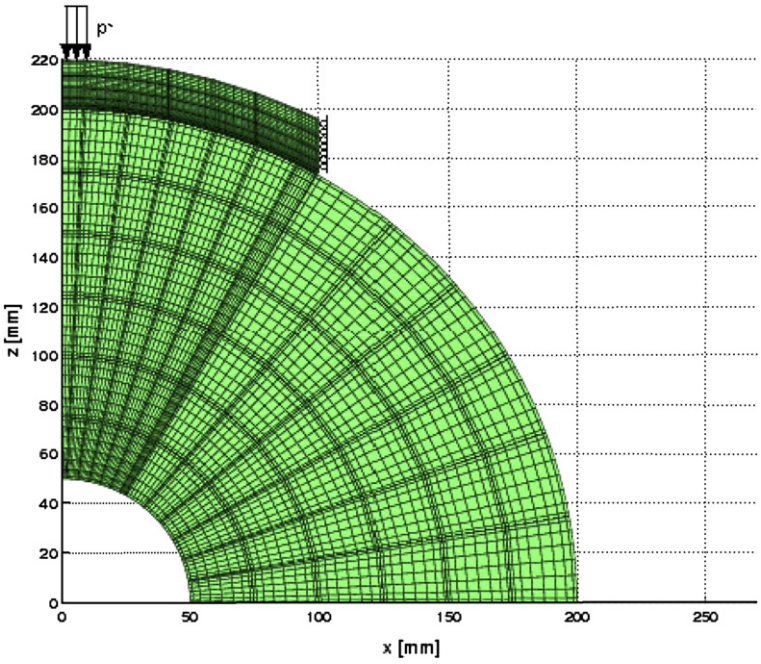

Fig. 9. Finite element mesh for half drum brake, $\tilde{p}$ =59.58333 MPa, resultant force $F_0 = 10$ kN.

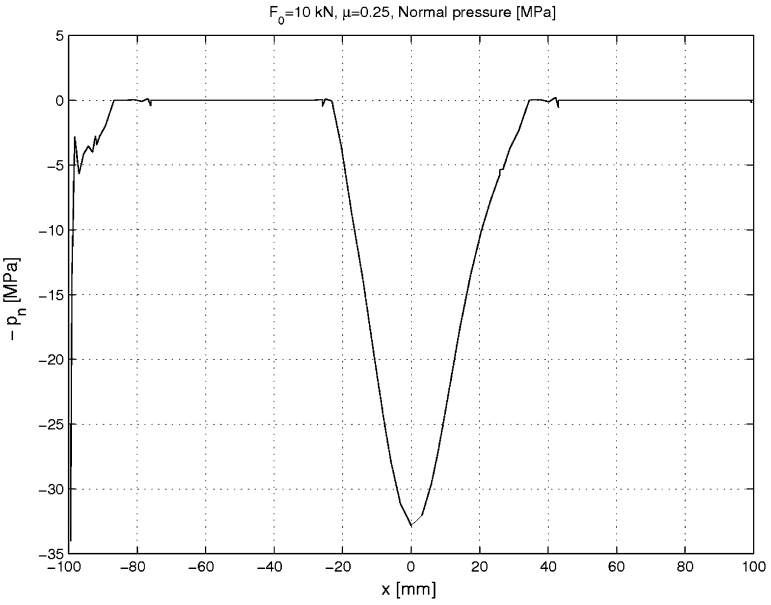

Fig. 10. Initial contact pressure at the contact surface.

at the bottom surface $z = 0$: $u = w = 0$. Here d_w denotes the displacement (or time) factor specifying the displacement values. The optimal shape of the contact surface can now be determined by assuming the optimal pressure distribution specified by (40). Assume $F_0 = 1$ kN, $M_0 = -5$ kN mm, $\mu = 0.25$. Fig. 14a presents the optimal contact shapes for several values of the displacement factors, that is the consecutive evolution of contact shape for increasing sliding displacements. Fig. 14b presents at the same displacement for the load

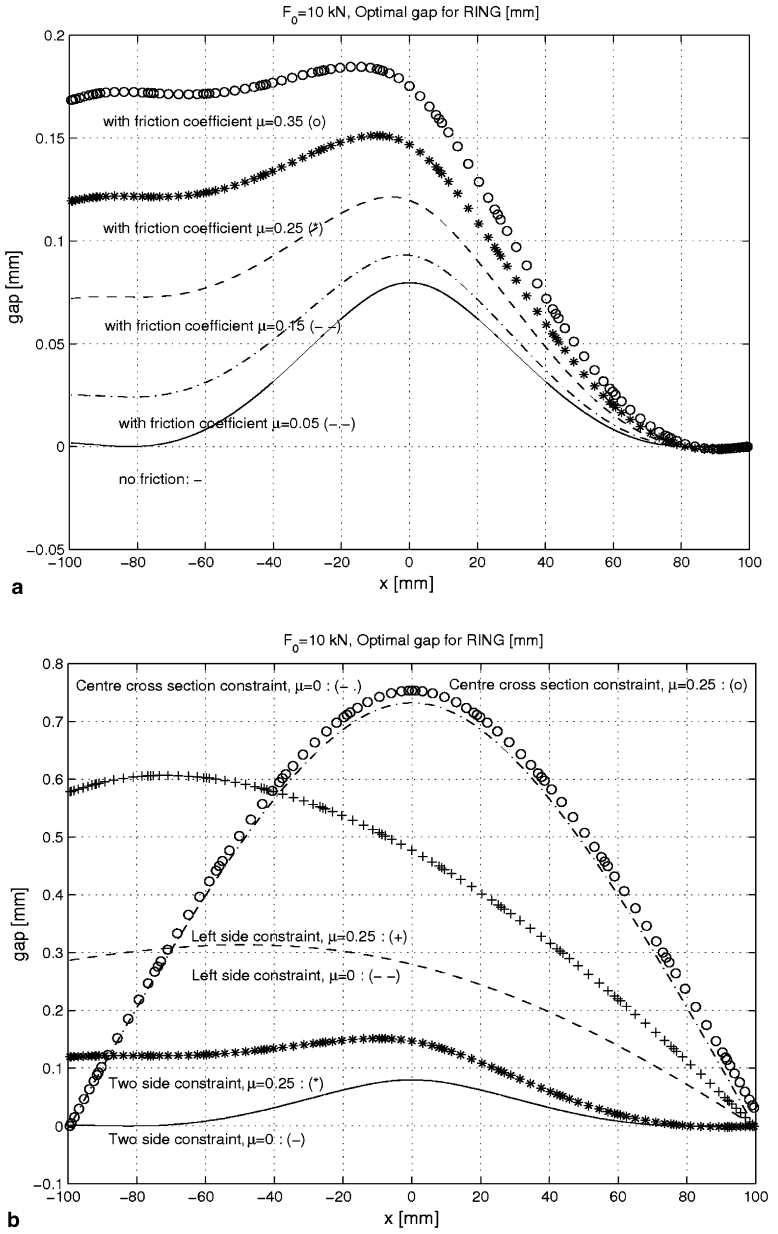

Fig. 11. Optimal wear profiles (normal initial gap) in the steady state: (a) constraint on both ends of the shoe, (b) the effect of tangential constraint on the form of optimal contact surface.

$F_0 = 1$ kN, $M_0 = 5$ kN mm, $\mu = 0.25$. Fig. 15a presents the optimal shape for the frictionless contact, for $F_0 = 1$ kN, $M_y = 0$ kN mm and Fig. 15b presents the optimal shapes for several values of the friction coefficient. It is seen that shape profiles are asymmetric with respect to punch center. Let us note that for the case of rotationally constrained punch, $\lambda_M = 0$, the solutions of Fig. 15 are valid as then $M_0 = 0$.

The present analysis generalizes the previous work by Marshek and Chen (1989) who integrated the wear rule with respect to the sliding distance to arrive at the steady state for the case $M_0 = 0$. Here, the steady state profiles are generated directly by applying the optimality conditions (40) for arbitrary values of normal force and moment at the contact surface. Figs. 16 and 17 present the distribution of normal stress σ_z within upper punch at the initial and optimal states. In Fig. 16 the initial stress field σ_z exhibits a singularity at the edge of

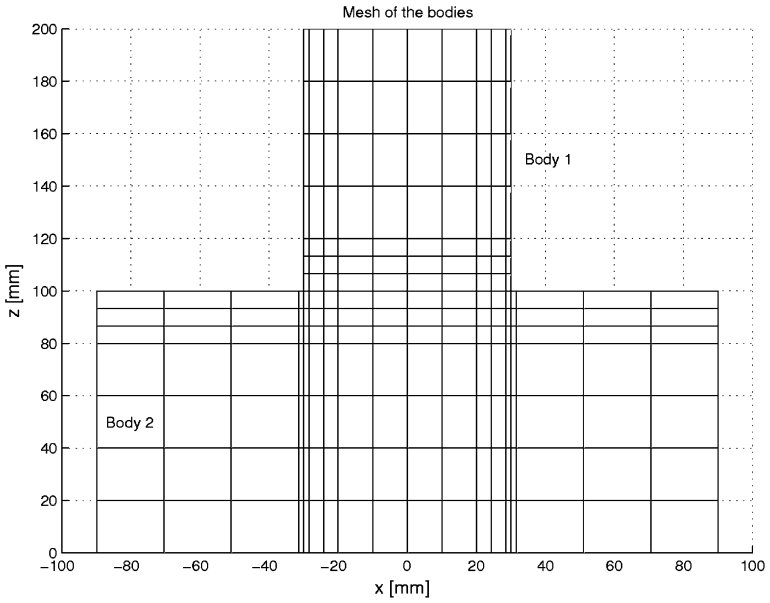

Fig. 12. Finite element of mesh of bodies.

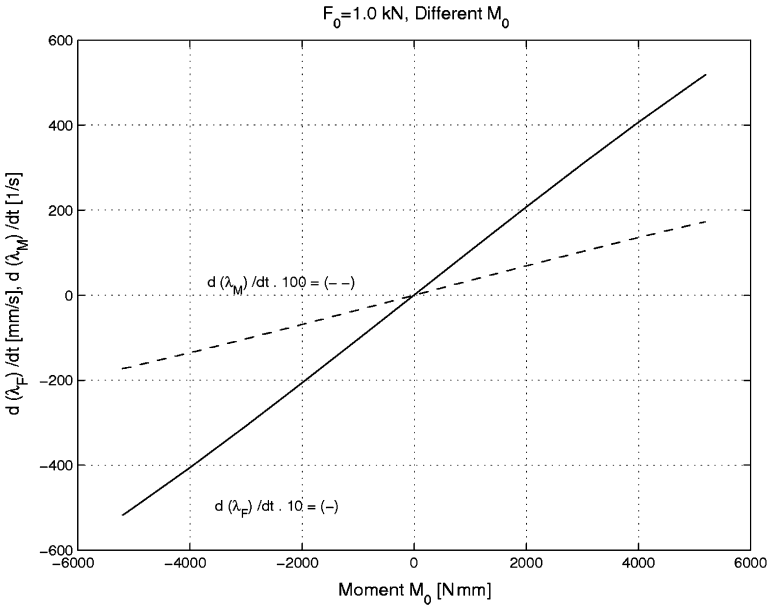

Fig. 13. Lagrangian multipliers (rates of translation and rotation) for varying moment M_0 and fixed normal force $F_0 = 1$ kN.

contact zone $z = 100$ mm, $x = 30$ mm and also at the boundary surface $z = 200$ mm, $x = \pm 30$ mm. The stress distribution at the optimal state is uniform at the contact surface, but stress singularity occurs at the loaded boundary.

Remark. Assume now that the wear process occurs also at the counterface Body 2. The value of wear in the steady state of the lower body can be calculated in the following way. Let the length of the contact zone be equal to L. The time period of contact of Body 1 in translating motion over a fixed point of contact surface of the lower body is $T_* = L/v_r$. The wear of Body 2 is calculated from the following time integral:

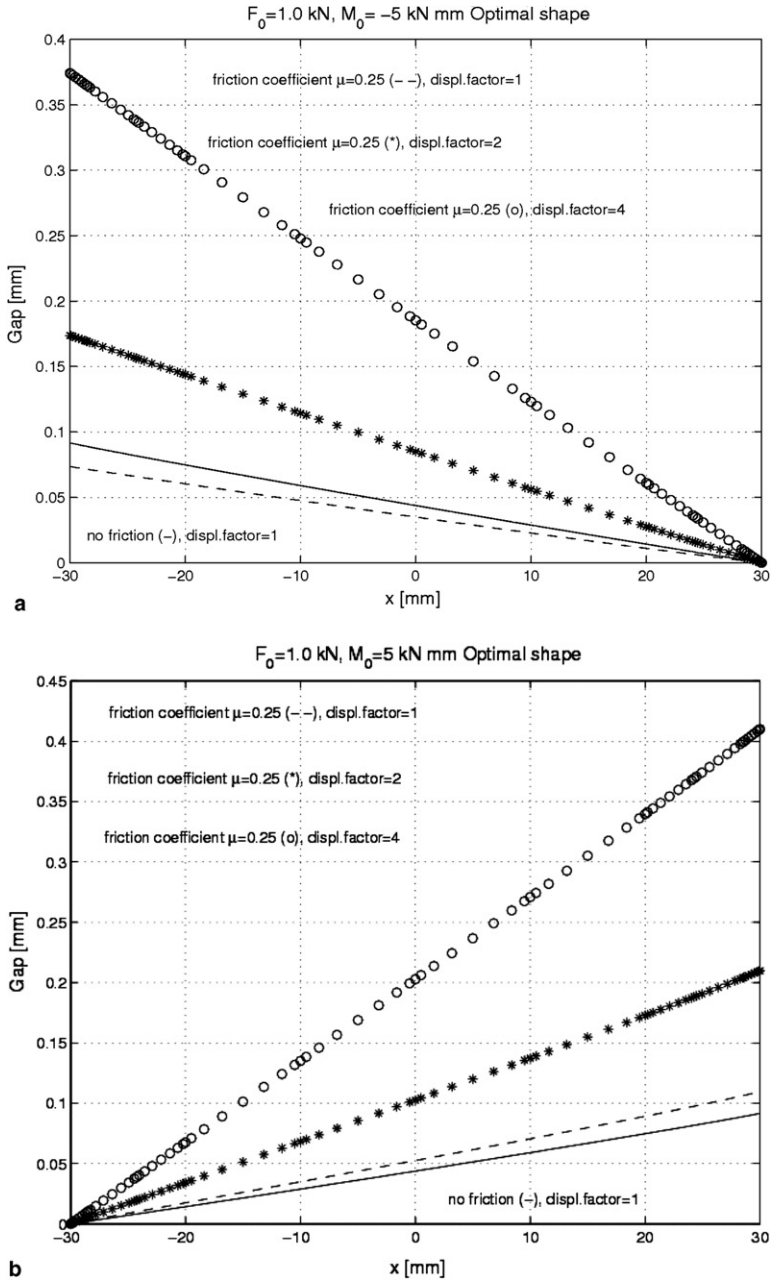

Fig. 14. Form of optimal contact shapes for two loading cases and varying sliding lengths, (a) $F_0 = 1$ kN, $M_0 = -5$ kN mm, $\mu = 0.25$, (b) $F_0 = 1$ kN, $M_0 = 5$ kN mm, $\mu = 0.25$.

$$w_2 = \int_0^{T_*} \tilde{\beta}_2 v_r^{a_2} p_n^b \left(x = \frac{L}{2} - v_r \tau \right) \mathrm{d}\tau. \tag{41}$$

Using the formula specifying contact pressure distribution for $q = 1$

$$p_n = \left\{ \frac{\dot{\lambda}_\mathrm{F} + \dot{\lambda}_M \left(\frac{L}{2} - v_r \tau \right)}{(b+1)(\tilde{\beta}_1 v_r^{a_1} + \tilde{\beta}_2 v_r^{a_2})} \right\}^{\frac{1}{b}}, \tag{42}$$

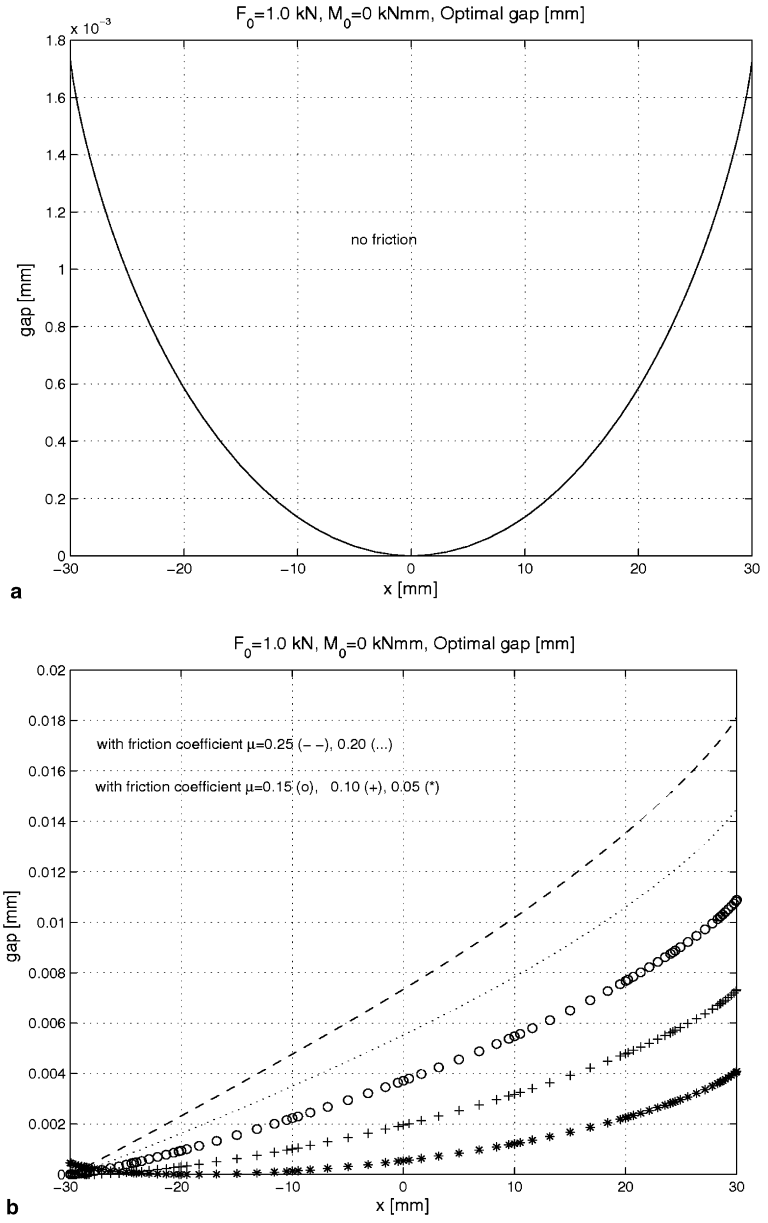

Fig. 15. Form of contact shapes for $M_0 = 0$, $\dot{\lambda}_M = 0$, $F_0 = 1$ kN and different friction conditions, (a) frictionless case, (b) varying friction coefficient.

we have the following result:

$$w_2 = \frac{\tilde{\beta}_2 v_r^{a_2}}{(b+1)(\tilde{\beta}_1 v_r^{a_1} + \tilde{\beta}_2 v_r^{a_2})} \frac{L}{v_r} \dot{\lambda}_{\mathrm{F}}. \tag{43a}$$

If $a = a_1 = a_2$, $\tilde{\beta}_1 = \tilde{\beta}_2$, then we have

$$w_2 = \frac{1}{2(b+1)} \frac{L}{v_r} \dot{\lambda}_{\mathrm{F}}. \tag{43b}$$

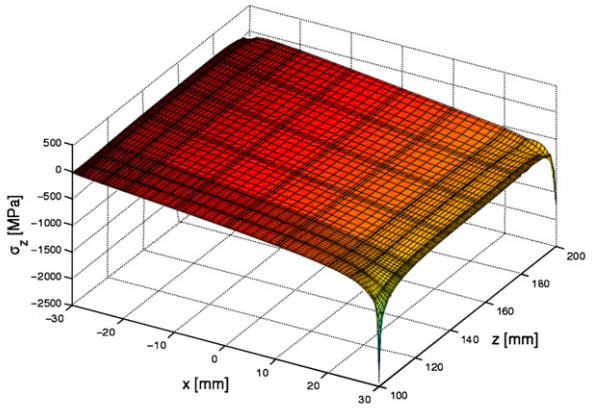

Fig. 16. Distribution of σ_z at the initial state (without friction and wear) at the load: $F_0 = 1$ kN, $M_0 = 5$ kN mm. At the end of contact zone $z = 100$, $x = 30$ we have singularity. At the same situation on the boundary $z = 200$, at the edge points the stress state has singularity.

7. Rotation with constant angular velocity: the case of annular punch

Consider the problem typical for disk brakes, namely the contact of two cylindrical bodies 1 and 2 with the annular punch 1 rotating uniformly with the angular velocity ω, Fig. 18. The internal and external radii of punch 1 are $r_i^{(1)}$, $r_e^{(1)}$ and its height is $h^{(1)}$. Similarly, the dimensions of body 2 are $r_i^{(2)}$, $r_e^{(2)}$, $h^{(2)}$. Assume the punch 1 to be loaded uniformly by the vertical traction $\sigma_z = -\tilde{p}$ on the upper surface. The resultant compressive force then equals $F_0 = \pi(r_e^2 - r_i^2)\tilde{p}$ and the slip velocity is $\|\dot{\mathbf{u}}_\tau\| = v_r = r\omega$ provided the body 2 is constrained and remains at rest.

Now the wear rate is

$$\dot{w}_i = \tilde{\beta}_i p_n^{b_i} v_r^{a_i} = \tilde{\beta}_i p_n^{b_i} (r\omega)^{a_i}, \quad i = 1, 2 \tag{44}$$

7.1. Variational principles

Because the punch is allowed to translate vertically along the rotation axis, we consider only normal force constraint. Following the analysis presented in Páczelt and Mróz (2005) we briefly present main formulae extending for two wear bodies.

Problem PW4: Minimizing the wear volume rate, let is define the objective integral as follows:

$$I_{\dot{W}}^{(q)} = 2\pi \int_{r_i}^{r_e} r^{\left(1 - \frac{aq}{bq-1}\right)} \mathrm{d}r \tag{45}$$

The optimal solution holds only in the case when $a_1 = a_2 = a$, $b_1 = b_2 = b$.

From the equilibrium equation it follows that

$$\dot{\lambda}_{\mathrm{F}} = \left\{ \sum_{i=1}^{2} \left(b(\tilde{\beta}_i \omega^a)^q A_i^{\frac{1-q}{q}} \right) \right\} \left(\frac{F_0}{I_{\dot{W}}^{(q)}} \right)^{bq-1} \tag{46}$$

and the optimal contact pressure distribution is

$$p_n = \left(\frac{F_0}{I_{\dot{W}}^{(q)}} \right) r^{-\frac{aq}{bq-1}} \quad \text{if } bq \neq 1 \tag{47}$$

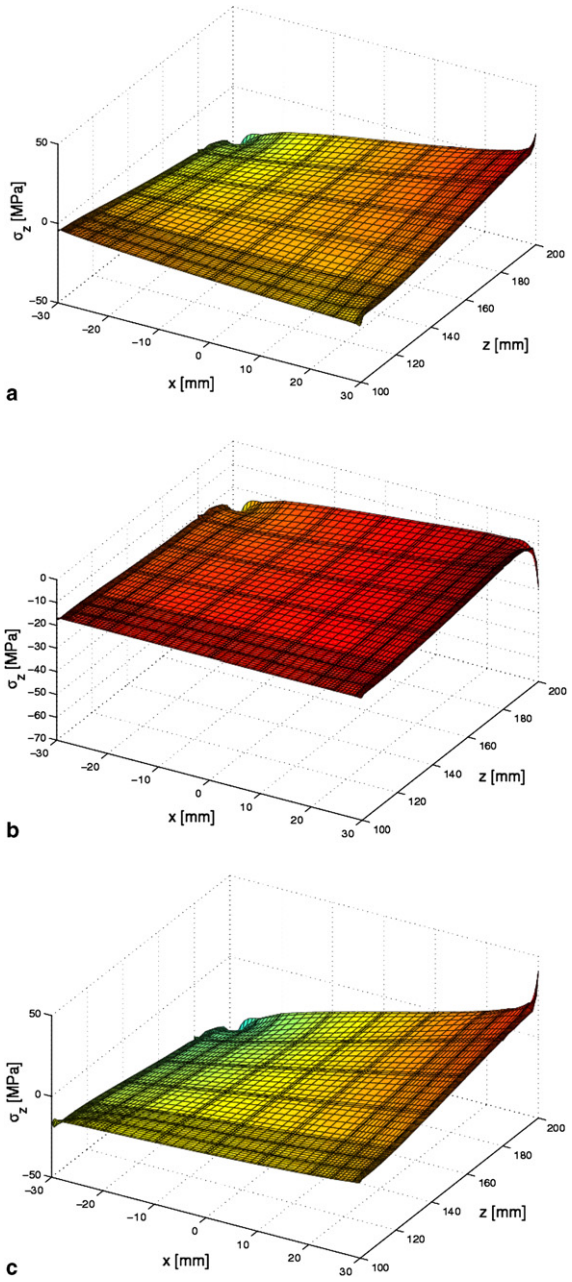

Fig. 17. Distribution of σ_z after optimization at the load: $F_0 = 1$ kN, (a) $M_0 = 5$ kN mm, (b) $M_0 = 0$ kN mm, (c) $M_0 = -5$ kN mm (in steady state of the wear process, $\mu = 0.25$).

The wear rate in this case varies along the radius, thus

$$\dot{w} = (\tilde{\beta}_1 + \tilde{\beta}_2)\omega^a \left(\frac{F_0}{I_{\dot{W}}^{(q)}}\right)^b r^{-\frac{a}{bq-1}} \quad \text{if } bq \neq 1 \tag{48}$$

The wear volume rate can be calculated very easily from the formula

$$\dot{W} = \int \dot{w}\,\mathrm{d}S = (\tilde{\beta}_1 + \tilde{\beta}_2)\omega^a \left(\frac{F_0}{I_{\dot{W}}^{(q)}}\right)^b 2\pi \int_{r_i}^{r_e} r^{\left(1-\frac{a}{bq-1}\right)}\,\mathrm{d}r = \dot{W}_{\dot{W}} \tag{49}$$

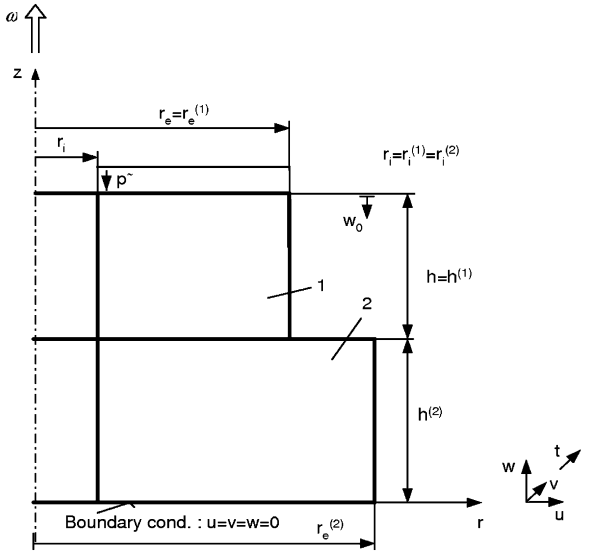

Fig. 18. The geometry of the annular punch problem.

Problem PW5: Minimizing the friction dissipation power, we have the following results

$$p_n = \left(\frac{F_0}{I_{D_\mathrm{F}}^{(q)}}\right) r^{-\frac{q}{q-1}} \quad \text{if } q \neq 1, \qquad I_{D_\mathrm{F}}^{(q)} = 2\pi \int_{r_i}^{r_e} r^{\left(1-\frac{q}{q-1}\right)}\,\mathrm{d}r$$

$$\dot{\lambda}_\mathrm{F} = \left((\mu\omega)^q B^{\frac{1-q}{q}}\right)\left(\frac{F_0}{I_{D_\mathrm{F}}^{(q)}}\right)^{q-1} \qquad \dot{w}_i = \tilde{\beta}_i \omega^{a_i}\left(\frac{F_0}{I_{D_\mathrm{F}}^{(q)}}\right)^{b_i} r^{\left(a_i-\frac{b_i q}{q-1}\right)}, \quad i = 1,2 \tag{50}$$

Problem PW6: By minimization of the wear dissipation power

$$D_\mathrm{w}^{(q)} = \sum_{i=1}^{2}\left(\int_{S_\mathrm{c}} (p_n \dot{w}_i)^q\,\mathrm{d}S\right)^{1/q} = \sum_{i=1}^{2}\left(\int_{S_\mathrm{c}} (\tilde{\beta}_i p_n^{b_i+1} v_r^{a_i})^q\,\mathrm{d}S\right)^{1/q} = \sum_{i=1}^{2} C_i^{1/q} \tag{51}$$

we obtain the following results:

Defining the Lagrangian function

$$L_{D_\mathrm{w}}^{(q)} = L_{D_\mathrm{w}}^{(q)}(p_n, \dot{\lambda}_\mathrm{F}) = D_\mathrm{w}^{(q)}(p_n) + \dot{\lambda}_\mathrm{F}\left(F_0 - \int_{S_\mathrm{c}} p_n\,\mathrm{d}S\right) \tag{52}$$

from the stationarity condition $\delta L_{D_\mathrm{w}}^{(q)} = 0 \Rightarrow$ we obtain the variational equation for the case $b_1 = b_2 = b$, thus

$$\int_{S_\mathrm{c}} \left\{\left[\sum_{i=1}^{2} C_i^{\frac{1-q}{q}} (\tilde{\beta}_i \omega^{a_i})^q (b+1) r^{q a_i}\right] p_n^{q(b+1)-1} - \dot{\lambda}_\mathrm{F}\right\} \delta p_n\,\mathrm{d}S = 0 \tag{53}$$

from which it follows that in order to have $\dot{\lambda}_\mathrm{F} = \text{const}$, there should be $a_1 = a_2 = a$.

In this case the contact pressure is

$$p_n = \left(\frac{F_0}{I_{D_\mathrm{w}}^{(q)}}\right)^{b} r^{-\frac{aq}{(b+1)q-1}} \quad \text{if } (b+1)q \neq 1, \tag{54}$$

where

$$I_{D_\mathrm{w}}^{(q)} = 2\pi \int_{r_i}^{r_e} r^{\left(1-\frac{aq}{(b+1)q-1}\right)}\,\mathrm{d}r \tag{55}$$

and the normal uniform translation velocity is

$$\dot{\lambda}_{\mathrm{F}} = \left\{ \sum_{i=1}^{2} \left((b+1)(\tilde{\beta}_i \omega^a)^q C_i^{\frac{1-q}{q}} \right) \right\} \left(\frac{F_0}{I_{D_{\mathrm{w}}}^{(q)}} \right)^{(b+1)q-1} \tag{56}$$

The wear rate is now calculated by the following formula:

$$\dot{w} = (\tilde{\beta}_1 + \tilde{\beta}_2)\omega^a \left(\frac{F_0}{I_{D_{\mathrm{w}}}^{(q)}} \right)^b r^{\left(a - \frac{abq}{(b+1)q-1} \right)} \tag{57}$$

The volume wear rate is

$$\dot{W} = \int \dot{w}\,\mathrm{d}S = (\tilde{\beta}_1 + \tilde{\beta}_2)\omega^a \left(\frac{F_0}{I_{\dot{W}}^{(q)}} \right)^b 2\pi \int_{r_i}^{r_e} r^{\left(1 + \frac{a(q-1)}{(b+1)q-1} \right)} \mathrm{d}r = \dot{W}_{D_{\mathrm{w}}} \tag{58}$$

It is important to note that for $q = 1$ the wear rate will be uniform along the contact surface. Thus the following theorem can be stated.

Theorem. *The steady state of wear process between two bodies in the relative rotation motion can be reached by minimizing the generalized wear dissipation power for* $q = 1$. *This result was established in* Páczelt and Mróz (2005). *Now we generalize it to the case of wear of two bodies.*

In this case, the contact pressure is

$$p_n = \frac{F_0}{I_{D_{\mathrm{w}}}^{(q=1)}} r^{-\frac{a}{b}} \tag{59}$$

and the local wear rate $\dot{w}$ expressed as follows:

$$\dot{w} = \left(\frac{F_0}{I_{D_{\mathrm{w}}}^{(q=1)}} \right)^b (\tilde{\beta}_1 + \tilde{\beta}_2)\omega^a = \mathrm{const} \tag{60}$$

The wear volume rate now is

$$\dot{W} = \int \dot{w}\,\mathrm{d}S = 2\pi \int_{r_i}^{r_e} \tilde{\beta}\omega^a \left(\frac{F_0}{I_{D_{\mathrm{w}}}^{(q=1)}} \right)^b r\,\mathrm{d}r = \tilde{\beta}\omega^a \left(\frac{F_0}{I_{D_{\mathrm{w}}}^{(q=1)}} \right)^b S_{\mathrm{c}} = \dot{W}_{D_{\mathrm{w}}}, \tag{61}$$

where $\tilde{\beta} = \tilde{\beta}_1 + \tilde{\beta}_2$.

Summarizing the result for Problems PW4, PW6 we can formulate the following conclusion.

The optimization Problems PW4, PW6 have solutions for the modified wear rule (4) only for equal parameters a_i $(a_1 = a_2)$ and b_i $(b_1 = b_2)$.

7.2. Analysis of singular solutions

Before we present numerical examples illustrating the evolution of regular to singular solutions, let us briefly discuss the singular stress distribution. For the problem PW4 of minimization of wear volume rate, from (47) it follows that

$$\frac{p_n}{p_{ni}} = \left(\frac{r_i}{r} \right)^{\frac{aq}{bq-1}}, \quad \frac{p_n}{p_{ne}} = \left(\frac{r}{r_e} \right)^{\frac{aq}{1-bq}} \tag{62}$$

where $p_{ni} = p_n(r_i)$ and $p_{ne} = p_n(r_e)$. Two different singular regimes are generated for

$$\begin{aligned} &bq > 1, \quad \text{and} \quad bq \to 1 \\ &bq < 1, \quad \text{and} \quad bq \to 1 \end{aligned} \tag{63}$$

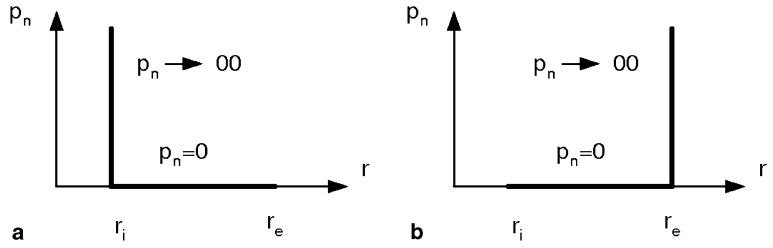

Fig. 19. Singular contact pressure regimes for (a) $bq > 1$, $bq \to 1$ and (b) $bq < 1$, $bq \to 1$.

The contact pressure is concentrated at the inner boundary for $bq > 1$, $bq \to 1$ and at the outer boundary for $bq < 1$, $bq \to 1$. Fig. 19 presents the singular pressure distribution. Similarly, for Problem PW5 (minimization of the friction dissipation power D_{F}), from (50) it follows that two singular regimes are generated for

$$q > 1, \quad q \to 1 \quad \text{and} \quad q < 1, \quad q \to 1 \tag{64}$$

Finally, for the problem PW6 (minimization of the wear dissipation power $D_{\mathrm{w}}^{(q)}$) the singular regimes are specified by the inequalities

$$(b+1)q > 1, \quad (b+1)q \to 1 \quad \text{and} \quad (b+1)q < 1, \quad (b+1)q \to 1 \tag{65}$$

and the singular pressure distribution is that presented in Fig. 19.

7.3. Comments on singular regimes

The punch is loaded by the constant pressure $\tilde{p}$ on its top surface in vertical direction, and the tangential displacement is $v_\varphi = r\omega t_*$, where t_* denotes time period from the initial instant. The contact shear stresses generate the torque

$$M_T = 2\pi \int_{r_i}^{r_e} \mu p_n r^2 \, \mathrm{d}r \tag{66}$$

and the friction dissipation power equals

$$D_{\mathrm{F}} = \int \mu p_n v_r \, \mathrm{d}S = \int \mu p_n r\omega \, \mathrm{d}S = 2\pi \int_{r_i}^{r_e} \mu p_n r^2 \, \mathrm{d}r\omega = M_T \omega \tag{67}$$

It is evident that the maximum of torque value is attained only when the outer punch contact perimeter ($r = r_e$) is in contact, and the minimum value occurs only when the inner contact perimeter ($r = r_i$) is in contact. Since the contact force is $F_0 = \pi(r_e^2 - r_i^2)\tilde{p}$, so the maximum and minimum torque values are

$$M_T^{\max} = r_e \mu F_0, \quad M_T^{\min} = r_i \mu F_0. \tag{68}$$

In this case the friction dissipation power may vary between the values

$$D_{\mathrm{F}}^{\min} = \omega M_T^{\min} = \omega r_i \mu F_0, \quad D_{\mathrm{F}}^{\max} = \omega M_T^{\max} = \omega r_e \mu F_0, \quad D_{\mathrm{F}}^{\min} \leqslant D_{\mathrm{F}} \leqslant D_{\mathrm{F}}^{\max} \tag{69}$$

It is important to note that the optimality condition of Problem PW5 implies that for $q > 1$, $q \to 1$ the singular solution converges to the state $D_{\mathrm{F}}^{\min}$ and for $q < 1$, $q \to 1$ the singular solution converges to the state $D_{\mathrm{F}}^{\max}$. The wear rate in these cases associated with singular pressure distribution has very high values, and the wear process does not reach a steady state.

7.4. Example 1: Singular optimal solutions for q = 1

To illustrate the transition to singular solutions let us consider the axisymmetric punch rotating with the angular velocity $\omega = 2.5$ rad/s. The radii of punch are $r_i = 20$ mm, $r_e = 120$ mm. The normal traction equals

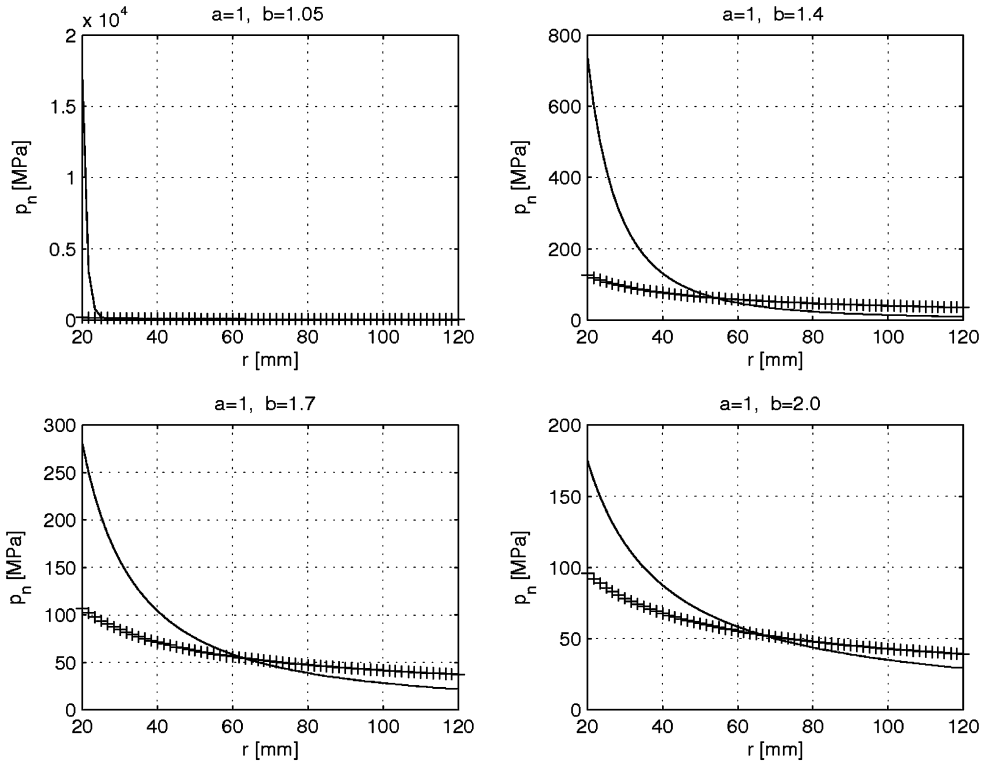

Fig. 20. Pressure distribution for $\min \dot{W}$ (−: continuous line) and for $\min D_{\mathrm{w}}$ (+: crossed line).

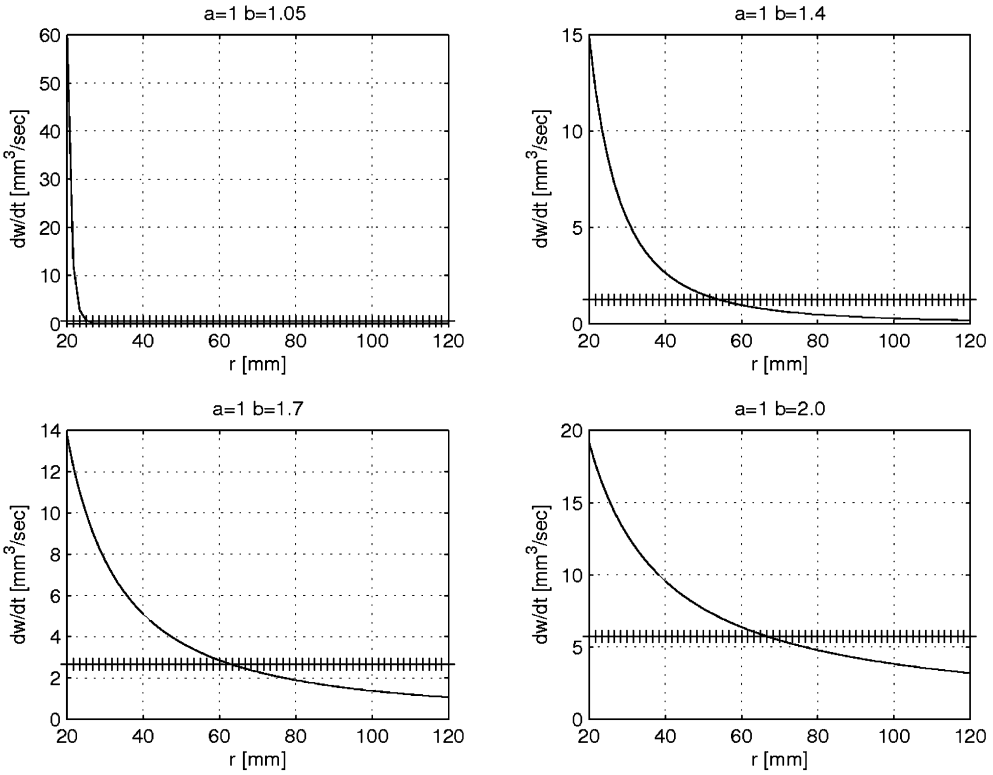

Fig. 21. Wear rate distribution at $\min \dot{W}$ (−: continuous line) and at $\min D_{\mathrm{w}}$ (+: crossed line).

$\tilde{p} = 100$ MPa, the coefficient of friction is $\mu = 0.25$. The wear parameters are $\beta = 0.0002$, $a = 1$, $b = 1.05, 1.2, \ldots, 2$. Fig. 20 presents the distribution of calculated pressure p_n generated by variational principles $\min \dot{W}(-)$ and $\min D_{\mathrm{w}}(+)$. We see that when $b \Rightarrow 1$, the condition $\min \dot{W}$ has no regular solution, and there is a singularity in the stress state.

For the condition $\min D_{\mathrm{w}}$ the wear rate $\dot{w}$ is uniform, but in the case $\min \dot{W}$ the corresponding wear rate is varying very rapidly along the radius of the punch (see Fig. 21).

The ratio of wear volume rates $w_r = \dot{W}_{\dot{W}}/\dot{W}_{D_{\mathrm{w}}}$ (see (49) and (61) for $q = 1$) for different b is

$b = 1.05$, $w_r = 0.3790$; $b = 1.2$, $w_r = 0.6209$; $b = 1.4$, $w_r = 0.8157$; $b = 1.6$, $w_r = 0.8957$;
$b = 1.7$, $w_r = 0.9173$; $b = 1.8$, $w_r = 0.9328$; $b = 1.9$, $w_r = 0.9442$; $b = 2.0$, $w_r = 0.9529$.

These results indicate that the condition $\min \dot{W}$ provides smaller wear volume rate than the condition $\min D_{\mathrm{w}}$.

7.5. Example 2: Effect of the control parameter q

Consider Problem PW6, namely minimization of $D_{\mathrm{w}}^{(q)}$ for the rotating punch with different values of the control parameter q. Let the wear parameters be $\beta = 0.0002$, $a = 1$, $b = 1$. The geometrical, material parameters are the same as in Example 1.

Fig. 22 presents the contact pressure distribution for different values of q. As was expected the contact pressure for $q = 0.5$ has the singularity at the radius $r_i = 20$ mm.

By selecting the value $q < 0.5$, we generate the singularity at the other boundary of the punch for $r_e = 120$ mm (see Fig. 23).

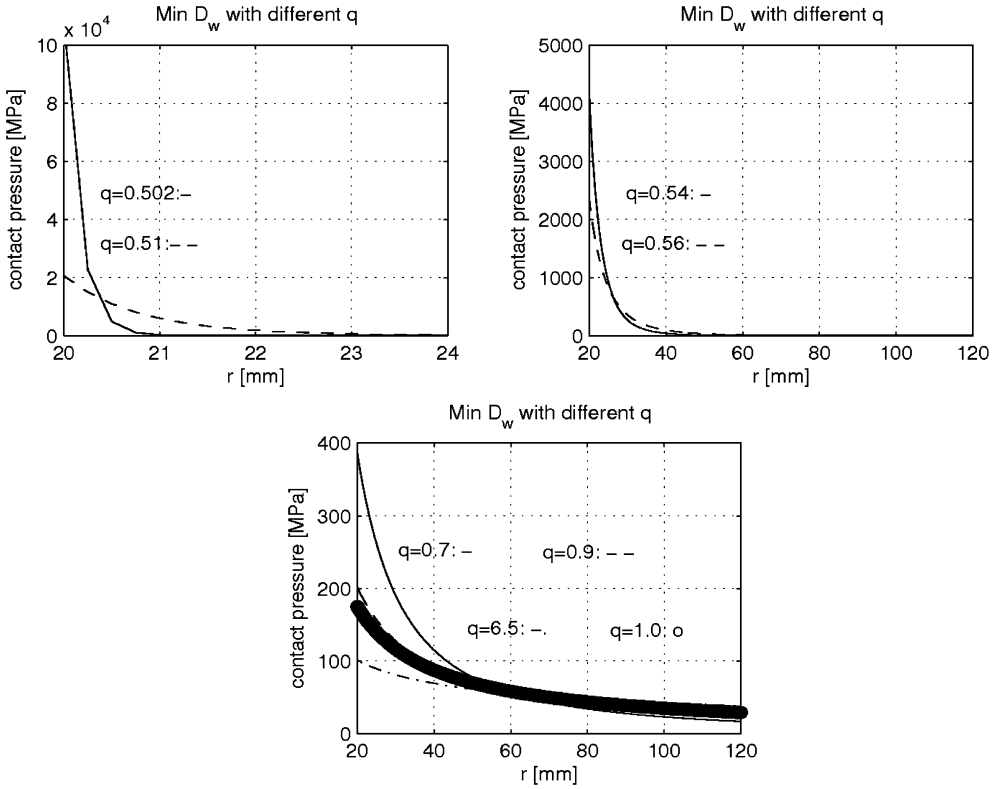

Fig. 22. The contact pressure distribution associated with the condition $\min D_{\mathrm{w}}$ for different values of the control parameter q.

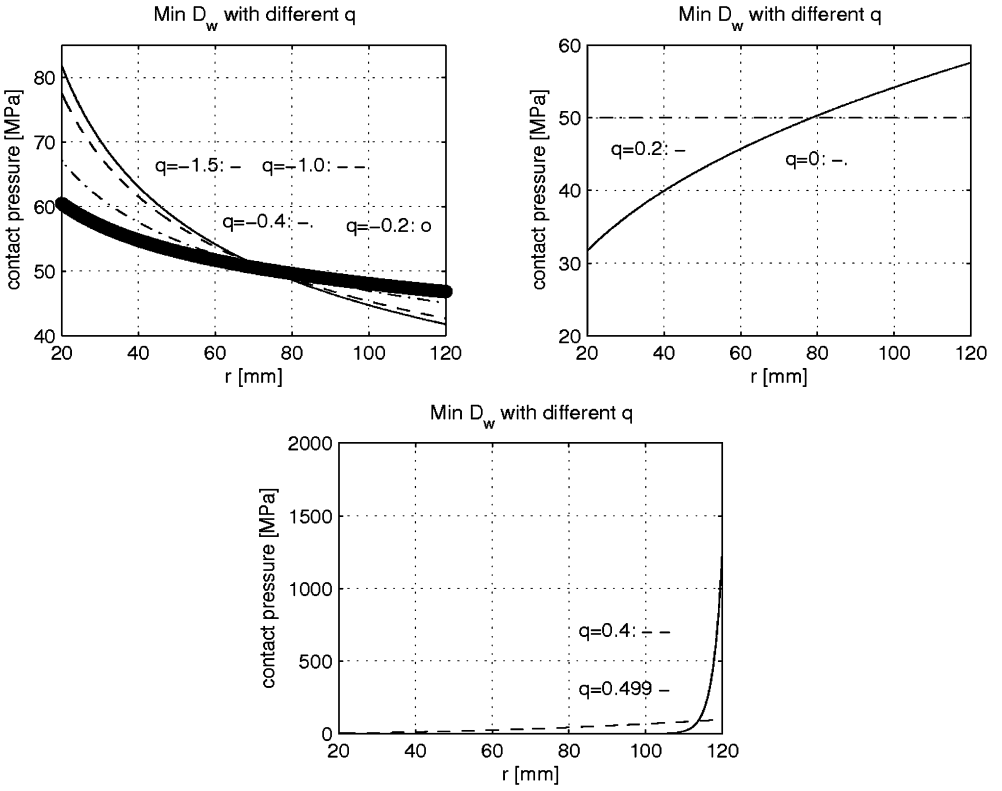

Fig. 23. The contact pressure distribution associated with the condition $\min D_w$ for varying values of the parameter q. The singular solution occurs at the external radius r_e.

Using the technique of contact pressure control (discussed in Appendices A and C of paper Páczelt and Mróz (2005)), the optimal shape of contact interface of punch 1 can easily be calculated.

Figs. 24 and 25 present the optimal gaps of the punch for $q > 0.5$ and $q < 0.5$ close to singular solutions. The finite element meshes are shown in Figs. 24a and 25a. It is seen that large shape gradients are generated near boundaries $r = r_i$ and $r = r_e$.

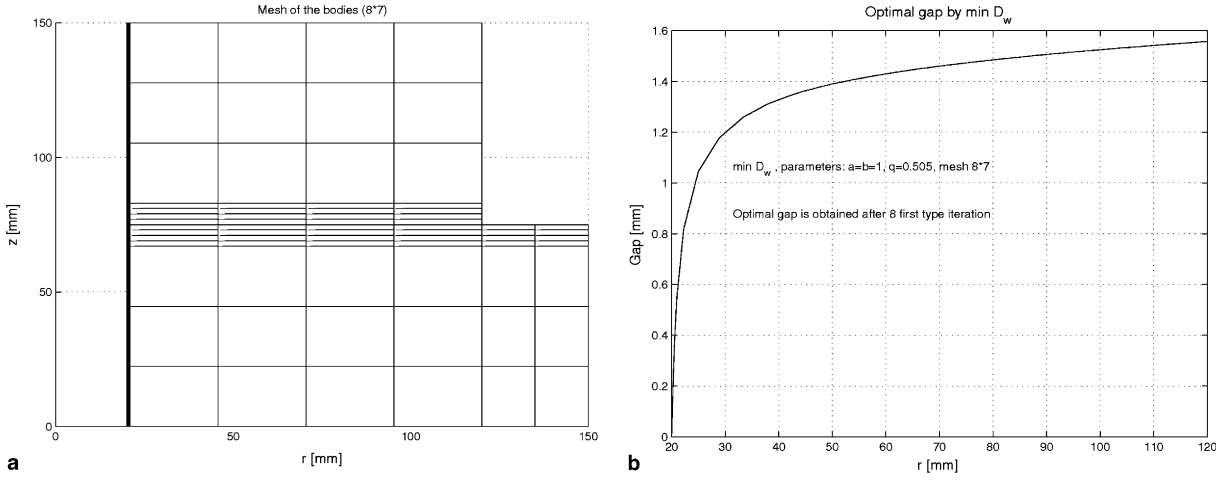

Fig. 24. The mesh of two bodies for the solution near the singular stress regime and the optimal shape of upper punch for $q = 0.505$.

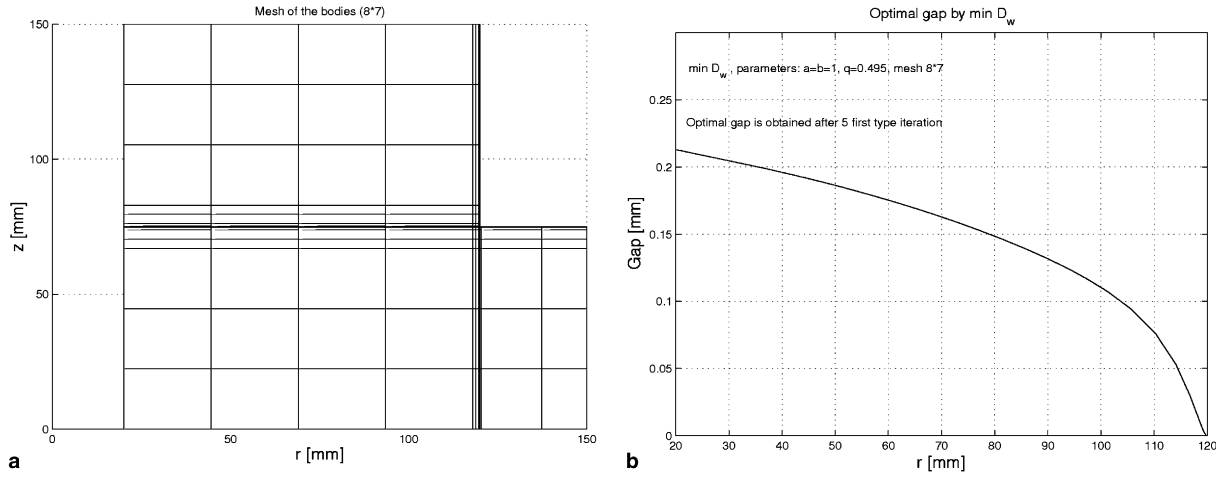

Fig. 25. The mesh of two bodies for the solution near-singular stress regime and the optimal shape of upper punch for $q = 0.495$.

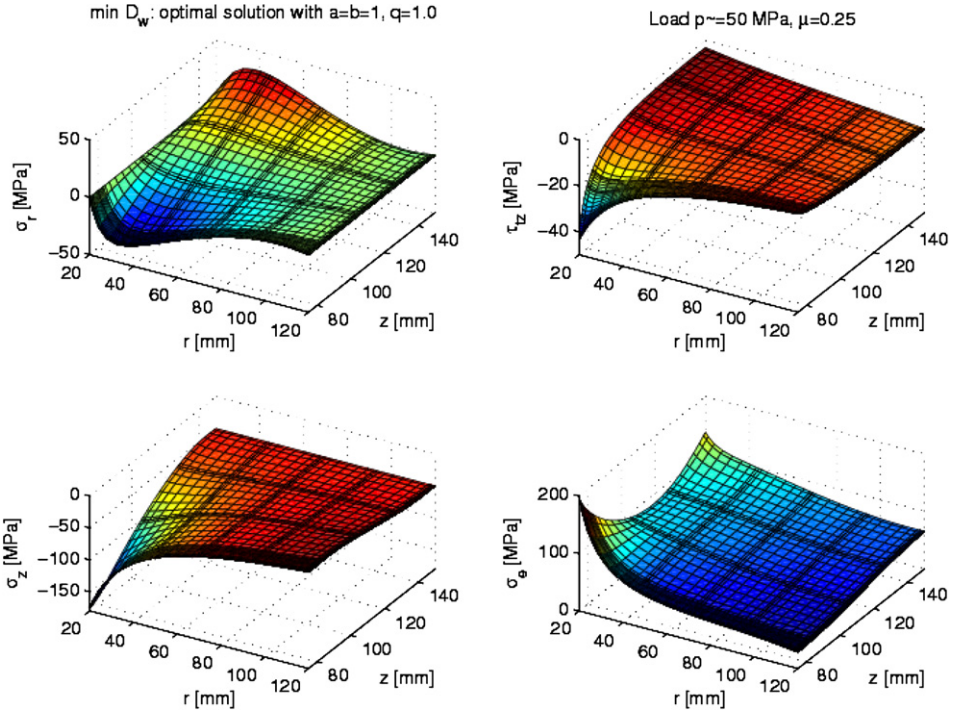

Fig. 26. Stress distribution in the upper punch at $q = 1$: σ_r – radial stress, σ_z – vertical stress, τ_{tz} – shear stress, σ_e – equivalent von Mises stress.

It is clear that the steady state wear process for optimal shapes of S_c shown in Figs. 24 and 25 cannot be attained. On the other hand, the uniform wear rate assuming the steady state can be generated for $q = 1$ by minimizing D_w. The optimal stress state and the corresponding shape of contact surface are shown in Figs. 26 and 27. The detailed analysis of this case was presented in the previous paper by Páczelt and Mróz (2005).

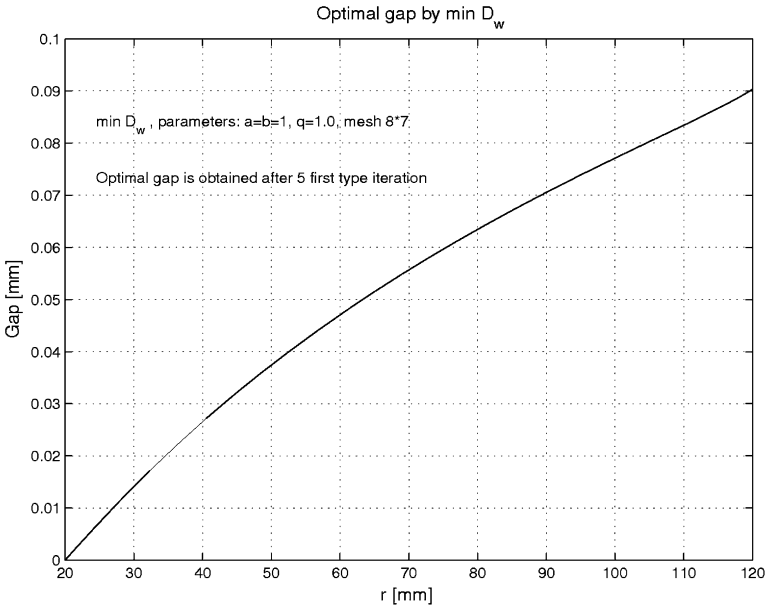

Fig. 27. Optimal shape of the contact surface of the upper punch corresponding to constant wear rate (obtained in five iterations).

8. Concluding remarks

In most papers published in the literature the contact shape evolution was studied by integrating incrementally the wear rule with account for contact pressure variation. The steady wear states were then reached asymptotically for very large number of time steps. Instead of such tedious procedure the present paper provides an alternative approach, namely, by deriving the optimality conditions for response functionals associated with the wear process. The optimal pressure distribution is then used in design of contact shape that could be reached in several iterations. It is believed that the present method provides a powerful tool in optimal contact shape design.

The minimization of three functionals was considered namely, generalized wear volume rate, generalized friction dissipation power and generalized wear dissipation power. The modified Archard wear rule was assumed and the optimality conditions were derived. It is assumed that wear parameters are different for each body. The respective optimality conditions provide different pressure distributions and local wear rate. In general, both regular and singular regimes of wear rate and pressure distribution may occur. The optimization problems are reduced to nonlinear programming problems and for their solution a special iteration procedure is used.

It is proved that a steady state wear process for two bodies in translatory motion is reached only when the wear parameters b_1, b_2 are equal in the modified Archard model $\dot{w}_i = \tilde{\beta}_i p_n^{b_i} v_r^{a_i}$, $i = 1,2$. In the case for rotary motion, the steady state is attained when $b_1 = b_2$, $a_1 = a_2$.

The wear process is analyzed in two specific cases. First, when the relative sliding velocity between bodies is constant and the second case, when one of bodies rotates with respect to the other body.

In the first case, the drum brake system and the translation of plane punch transferring normal force and moment was analyzed. It was proved, that the steady state of wear process in the drum brake system may be reached when the control parameter $q \to \infty$, however for translation on plane surface, the steady state is reached is for $q = 1$.

The convergence of solution is most pronounced to the uniform wear and pressure distribution in the case of minimization of the wear dissipation power. Due to effect of friction forces at the contact the optimal gap shape is not symmetrical with respect to z-axis.

In the plane punch problem the steady state profiles are directly generated by applying the optimality conditions for contact pressure distribution for arbitrary values of normal force and moment at the contact

surface. Using the special iteration technique (discussed in Appendices A and C of paper Páczelt and Mróz (2005)), the optimal shape of contact interface of Body 1 can easily be calculated. In this case the bodies ($i = 1,2$) in the contact surface S_c are loaded by optimal contact pressure p_n and shear stress $\tau_{xz}^{(i)} = (-1)^i \mu p_n$, $i = 1,2$ consistently with the orientation of relative velocity v_r.

In the second case of punch rotation the steady state condition of wear process is reached for a minimum of wear dissipation power, $q = 1$, and the corresponding optimal pressure distribution. The optimal or steady state shape can be obtained through the optimization procedure based on required pressure distribution using the pressure control technique. The minimization of volume wear rate provides the solution corresponding to smaller wear volume than for the case of minimization of the wear dissipation power, but this optimal solution does not generate steady state.

The singular solutions in both cases correspond to large contact pressure values at the perimeter or center line of contact surface. These solutions do not generate steady state wear regimes. However, they may be applied when the short period response is of interest. In practical applications the imposed stress constraints can modify these singular solutions and provide regular contact pressure distributions.

Acknowledgements

The present research was partially supported by the Hungarian Academy of Sciences, by grant OTKA T037759 and by the Polish Ministry of Education and Science, Grant No. 3 T08C 02129.

Appendix A. Iterative solution of optimal contact shape problem

The iterative scheme for contact shape optimization was discussed in detail by Páczelt (2000). Here we only outline the consecutive steps.

The iterative process proceeds according to the following scheme:

1. Solution of the original contact problem: specification of contact pressure $p_n^{(0)} = p_n^{(0)}(s)$, $p_{\max}^{(0)}$, $s = R\alpha$, $k = 0$
2. $k = k + 1$
3. Assume the controlled pressure distribution according to $v(s) = 1$

   $$p_n^{(k)}(s) = v(s)p^*.$$

   Consider first the displacement induced loading. The value of the parameter p^* is obtained from the contact problem solution at the previous iterative step $k - 1$,

   $$p^* = \max p_n^{(k-1)}(s).$$

   For the case of traction the solution of contact problem is not required. The value of p^* at each step is specified from the load equilibrium condition, thus

   $$F_0 = p^* \int_{-\alpha_o}^{\alpha_o} (\cos\alpha + \mu \sin\alpha) R \, \mathrm{d}\alpha,$$

   where μ – coefficient of friction.
4. The separated bodies are now loaded by the pressures $p_n^{(k)}(s)$ and $-p_n^{(k)}(s)$ and in the case frictional contact also by shear stresses $\mu p_n^{(k)}(s)$ and $-\mu p_n^{(k)}(s)$ in the tangential direction at the contact surface S_c and displacements $u_n^{(1)}$ and $u_n^{(2)}$ are determined
5. Calculate the discontinuity of normal displacements

   $$m(s) = u_n^{(1)} - u_n^{(2)} = [u_n]$$

6. Specify the minimal value $\min m(s) = m(s_*)$ and "rigid displacement" $\Delta = m(s_*)/\cos\alpha_*$, where α_* – the central angle of contact point with coordinate s_*
7. Generate the new initial gap:

   $$g(s) = m(s) - \Delta \cdot \cos\varphi(s) \Rightarrow g(\mathbf{x})$$

References

Goryacheva, I.G., Dobuchin, M.H., 1988. Contact Problems in Tribology. Mashinostroenie, Moscow (in Russian).
Haslinger, J., Neittaanmaki, P., 1988. Finite Element Approximation for Optimal Shape Design. John Wiley & Sons Ltd., London.
Hilding, D., Klarbring, A., Petterson, J., 1999. Optimization of structures in unilateral contact. ASME Appl. Mech. Rev. 52 (4), 139–160.
Ireman, P., Klarbring, A., Strömberg, N., 2002. Finite element algorithms for thermoelastic wear problems. Eur. J. Mech. A/Solids 21, 423–440.
Johansson, L., 1994. Numerical simulation of contact pressure evolution in fretting. J. Tribol. 116, 247–254.
Kalker, J.J., 1985. A course of contact mechanics. a79C, Delft University of Technology, Delft.
Kim, H.K., Won, D., Burris, D., Holtkamp, B., Gessel, G.R., Swanson, P., Sawyer, W.G., 2005. Finite element analysis and experiments of metal/metal wear in oscillatory contacts. Wear 258, 1787–1793.
Laursen, T.A., 2002. Computational Contact and Impact Mechanics. Springer-Verlag, Berlin.
Marshek, K.M., Chen, H.H., 1989. Distribution pressure wear theory for bodies in sliding contact. J. Tribol. (ASME) 111, 95–100.
Mróz, Z., Stupkiewicz, S., 1994. An anisotropic friction and wear model. Int. J. Solids Struct. 31, 1113–1131.
Páczelt, I., 2000. Iterative methods for solution of contact optimization problems. Arch. Mech. 52 (4–5), 685–711.
Páczelt, I., Baksa, A., 2002. Examination of contact optimization and wearing problems. J. Comput. Appl. Mech. 3 (1), 61–84.
Páczelt, I., Mróz, Z., 2005. On optimal contact shapes generated by wear. Int. J. Numer. Methods Eng. 63, 1310–1347.
Páczelt, I., Pere, B., 1999. Investigation of contact wearing problems with *hp*-version of the finite element method. In: Skrzypek, J.J., Hetnarski, R.B. (Eds.), Proceedings Thermal Stress'99, 13–17 June 1999, Cracow, Poland. Cracow University of Technology, pp. 81–84.
Páczelt, I., Szabó, T., 1994. Optimal shape design for contact problems. Struct. Optimiz. 7 (1/2), 66–75.
Páczelt, I., Szabó, T., 2002. Solution of contact optimization problems of cylindrical bodies using hp-FEM. Int. J. Numer. Methods Eng. 53, 123–146.
Strömberg, N., 1998. Finite element treatment of two-dimensional thermoelastic wear problems. Comput. Methods Appl. Mech. Eng. 177, 441–455.
Strömberg, N., Johansson, L., Klarbring, A., 1996. Derivation and analysis of a generalized standard model for contact, friction and wear. Int. J. Solids Struct. 33, 1817–1836.
Stupkiewicz, S., Mróz, Z., 1999. A model of third body abrasive friction and wear in hot metal forming. Wear 231, 124–138.
Szabó, B., Babuska, I., 1991. Finite Element Analysis. Wiley-Intersience, New York.
Wriggers, P., 2002. Computational Contact Mechanics. J. Wiley Sons, New York.
Wriggers, P., Miehe, C., 1994. Contact constraints within thermomechanical analysis – a finite element model. Comput. Methods Appl. Mech. Eng. 113, 301–319.